Article

Serotonergic Modulation of Walking in *Drosophila*

Graphical Abstract

Highlights

- Serotonergic neurons in the fly VNC extensively innervate the leg neuropils

- Activating these neurons causes flies to walk slower but maintain coordination

- Silencing these neurons causes flies to walk faster in many contexts

- Silencing these neurons alters how flies respond to being startled

Authors

Clare E. Howard, Chin-Lin Chen, Tanya Tabachnik, Rick Hormigo, Pavan Ramdya, Richard S. Mann

Correspondence

rsm10@columbia.edu

In Brief

Howard et al. describe the role of the neuromodulator serotonin in modifying *Drosophila* walking behavior. Serotonin release in the ventral nerve cord serves to slow walking speed, regardless of the context. Serotonin-mediated slowing of walking speed is required for a normal response to being startled by a novel stimulus.

CellPress

Current Biology
Article

CellPress

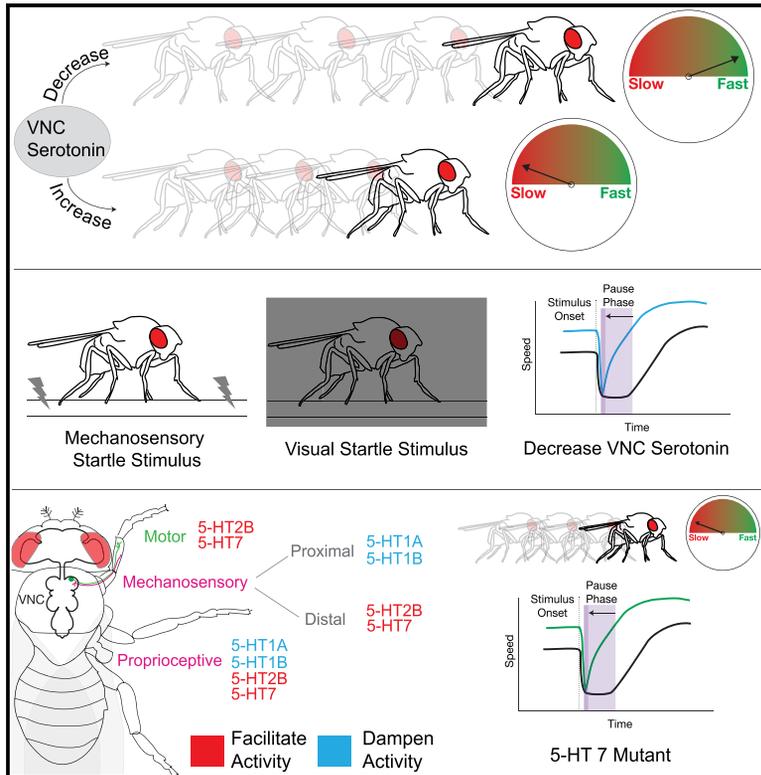# Serotonergic Modulation of Walking in *Drosophila*

Clare E. Howard,[1,2] Chin-Lin Chen,[3,4] Tanya Tabachnik,[5] Rick Hormigo,[5] Pavan Ramdya,[3,4] and Richard S. Mann[1,6,7,*]
[1]Mortimer B. Zuckerman Mind Brain Behavior Institute, Columbia University, New York, NY 10027, USA
[2]Medical Scientist Training Program, Columbia University, New York, NY 10027, USA
[3]Brain Mind Institute, Ecole Polytechnique Federale de Lausanne, CH-1015 Lausanne, Switzerland
[4]Interfaculty Institute of Bioengineering, Ecole Polytechnique Federale de Lausanne, CH-1015 Lausanne, Switzerland
[5]Advanced Instrumentation Group, Zuckerman Mind Brain Behavior Institute, Columbia University, New York, NY 10027, USA
[6]Departments of Biochemistry and Molecular Biophysics and Neuroscience, Columbia University, New York, NY 10027, USA
[7]Lead Contact
*Correspondence: rsm10@columbia.edu
https://doi.org/10.1016/j.cub.2019.10.042

SUMMARY

To navigate complex environments, animals must generate highly robust, yet flexible, locomotor behaviors. For example, walking speed must be tailored to the needs of a particular environment. Not only must animals choose the correct speed and gait, they must also adapt to changing conditions and quickly respond to sudden and surprising new stimuli. Neuromodulators, particularly the small biogenic amine neurotransmitters, have the ability to rapidly alter the functional outputs of motor circuits. Here, we show that the serotonergic system in the vinegar fly, *Drosophila melanogaster*, can modulate walking speed in a variety of contexts and also change how flies respond to sudden changes in the environment. These multifaceted roles of serotonin in locomotion are differentially mediated by a family of serotonergic receptors with distinct activities and expression patterns.

INTRODUCTION

Insects have a remarkable capacity to adapt their locomotor behaviors across a wide range of environmental contexts and to confront numerous challenges. They can walk forward, backward, and upside down, navigate complex terrains, and rapidly recover after injury [1–7]. To achieve this wide range of behaviors, insects regulate their walking speed and kinematic parameters, allowing them to modify stereotyped gaits as needed [3, 7–10]. Because overlapping sets of motor neurons and muscles are recruited for all of these behaviors, animals must be able to rapidly modulate the circuit dynamics that control locomotor parameters [11, 12].

As with limbed vertebrates, most insects use multi-jointed legs to walk [11, 13]. In the vinegar fly, *Drosophila melanogaster*, the neural circuits that orchestrate complex walking gaits are located in the ventral nerve cord (VNC), a functional analog of the vertebrate spinal cord that includes three pairs of thoracic neuromeres (T1, T2, and T3) that coordinate the movements of three corresponding pairs of legs [14–17]. The VNC receives descending commands from the brain and sends motor output instructions via motor neurons to peripheral musculature [17–19].

Sensory neurons, which convey proprioceptive and tactile information, project axons from the appendages to the VNC by these same fiber tracts, where they arborize in the leg neuropils [20–24] (Figure 1A). Notably, the VNC is capable of executing coordinated leg motor behaviors, such as walking and grooming, even in decapitated animals [26]. Thus, as has been described in other insects, the VNC likely harbors neural networks that can drive the coordinated flexion and extension of each leg joint and also coordinated walking gaits [11, 27].

Numerous studies have established that sensory input from the legs is required for robust and stereotyped locomotor patterns, regulating the timing, magnitude, and coordination of locomotor activity [5, 10, 13, 23, 25, 28–30]. However, sensory feedback cannot be the only means for tuning locomotion: mutation of proprioceptive receptors or even deafferenting limbs does not block coordinated walking [25, 31–35]. Beyond sensory feedback-driven tuning of gait patterns, larger behavioral changes must be accomplished by other circuits. These likely include neuromodulatory systems, including the mono-amines dopamine, norepinephrine, and serotonin, which are highly conserved throughout the animal kingdom [36–38].

Monoamines have been shown to modulate, and even induce, the activities of central pattern generating (CPG) motor circuits. In crustaceans, neuromodulation causes the gastric CPG to generate distinct rhythmic activity patterns from the same neural network to address distinct behavioral demands [36, 39]. Remarkably, the same neuromodulatory systems appear to play similar roles across species. Serotonin has been shown to slow locomotor rhythms in animals as diverse as the lamprey, cat, and locust [40–42]. In *Drosophila*, monoamine neurotransmitters have also been shown to modulate a wide range of behaviors. In addition to slowing walking speed, serotonin modulates sleep, aggression, and anxiety-related motor behaviors [43–49]. Dopamine, in contrast, has been linked to hyperactivity [26, 50–52]. Octopamine has been shown to mediate starvation-induced hyperactivity, and in its absence animals walk more slowly [10, 53, 54]. As each of these neuromodulatory systems plays a variety of roles in regulating complex behaviors, it has thus far been challenging to tease apart which of the effects on walking behavior are due to direct modulation of motor circuitry or are a secondary consequence of modulating higher-order circuits in the brain.

In this work, we show that the serotonergic neurons within the VNC have the ability to modulate walking speed in multiple internal states and many environmental contexts, as well as in
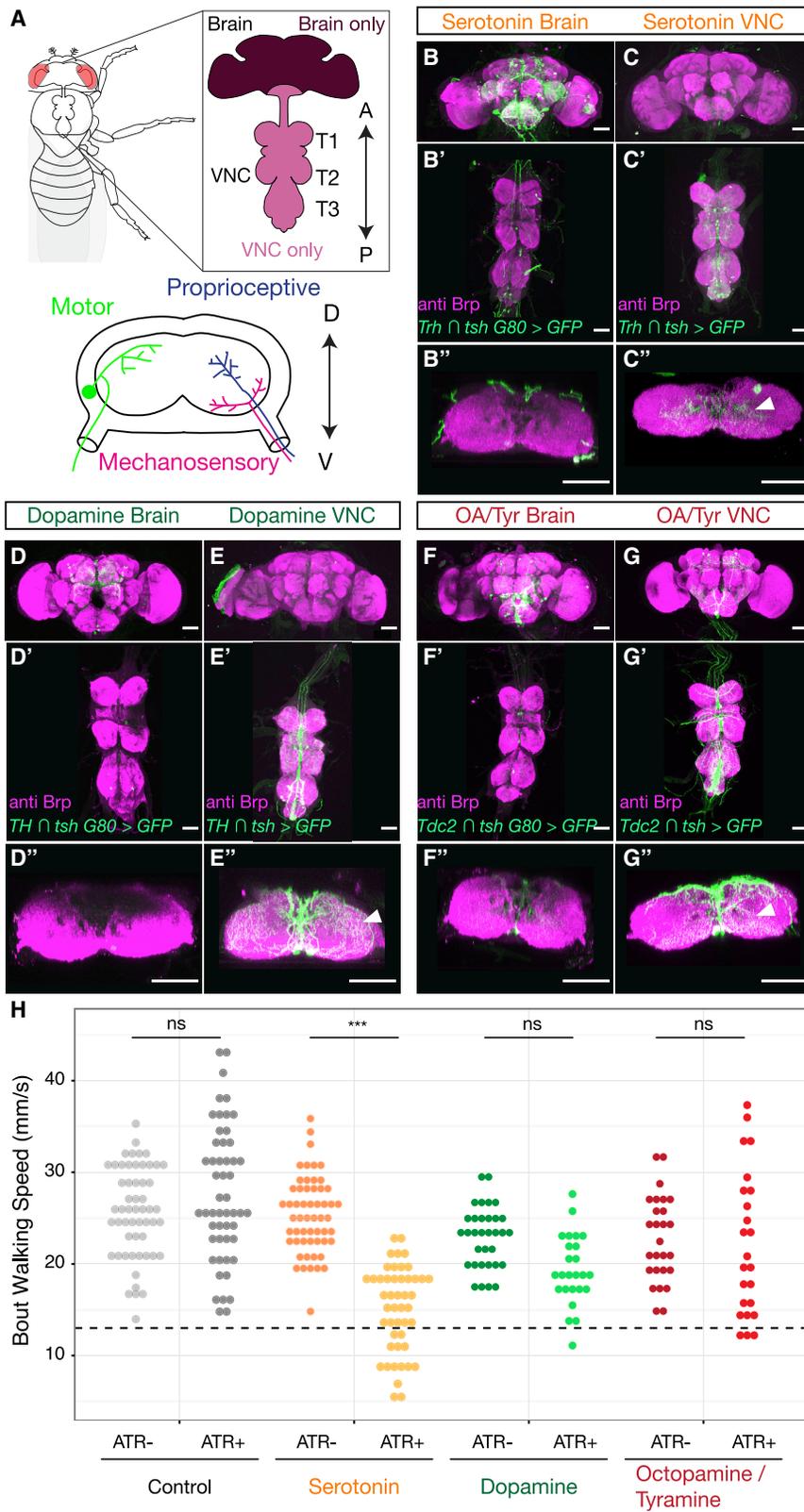
Figure 1. Neuromodulators in the *Drosophila* CNS

(A) The adult *Drosophila* CNS is composed of the brain and the VNC, which consists of three pairs of thoracic neuropils (T1, T2, and T3), each of which corresponds to a pair of adult legs, and an abdominal ganglion. The anterior (A)-posterior (P) axis is specified. Lower panel: cross-section of a thoracic neuropil illustrating projections of locomotor circuit components, including motor neurons, and sensory neurons that convey mechanosensory and proprioceptive information from the legs. The dorsal (D)-ventral (V) axis is specified.

(B–G) Maximum intensity projections show the expression patterns driven by Gal4 lines labeling either brain-derived (B, D, F, *Gal4* intersected with *tsh Gal80*) or VNC-derived (C, E, G, *Gal4* intersected with *tsh*) serotonergic (B and C, *Trh Gal4*), dopaminergic (D and E, *TH Gal4*), or octopaminergic/tyraminergic (OA/Tyr) (F and G, *Tdc2 Gal4*) neurons. (B″–G″) Projection of a subset of cross sections of the VNC shows innervation of the T1 neuropil. Arrowheads point to innervation in the leg neuropils. All scale bars are 50 μm.

(H) Optogenetic activation of serotonergic (*Trh ∩ tsh > csChrimson*) neurons in the *Drosophila* VNC but not dopaminergic (*TH ∩ tsh > csChrimson*) or octopaminergic/tyraminergic (*Tdc2 ∩ tsh > csChrimson*) neurons slows walking speed compared to all-trans-retinal (ATR) negative and non-Gal4 ($w^{1118} ∩ tsh > csChrimson$) controls. These experiments were carried out using the Flywalker assay ([25]; see Figure S3A for a schematic). $*p < 0.05$ $**p < 0.01$ $***p < 0.001$ by Kruskal-Wallis test with Dunn-Sidak correction for multiple comparisons. n = walking bouts (recorded from N animals) w^{1118} ATR⁻ 55 (14–31); w^{1118} ATR⁺ 52 (14–36); *Trh* ATR⁻ 56 (12–30); *Trh* ATR⁺ 47 (10–23); *TH* ATR⁻ 33 (10–24); *TH* ATR⁺ 25 (10–26); *Tdc2* ATR⁻ 27 (10–27); *Tdc2* ATR⁺ 24 (10–25).

See also Figure S1.

response to startling stimuli. Additionally, we demonstrate that these modulatory effects are enacted through serotonin's action on specific receptors that are expressed in different parts of the locomotor circuit. Together, these findings reveal that neuromodulatory systems regulate multiple aspects of walking behavior, helping animals to effectively respond to rapidly changing environments.

RESULTS

VNC Serotonergic Neurons Arborize within the Leg Neuropils

To identify neuromodulatory neurons that might play a role in modulating walking behavior, we drove expression of a fluorescent reporter with Gal4 under the control of promoters encoding key synthetic enzymes for each neuromodulatory system—*Tryptophan hydroxylase* (*Trh* for serotonin (5-HT) [48]); *tyrosine hydroxylase* (*TH* or *ple* (*pale*) for dopamine [55]); and *Tyrosine decarboxylase 2* (*Tdc2* for octopamine and tyramine [56]). All of these drivers show extensive expression in cells both within the VNC and the brain, with processes that densely innervate VNC leg neuromeres (Figure 1).

To determine whether local neuromodulatory VNC neurons or descending neurons originating in the brain innervate the leg neuropils, we used genetic intersectional tools to limit the expression of these Gal4 lines to either the brain or VNC (Figure 1A) (see STAR Methods). These experiments show that neuromodulatory innervation of the leg neuropils arises almost entirely from VNC interneurons and not from descending neurons in the brain (Figures 1B–1G). Moreover, these VNC neurons extensively innervate the leg neuropils. Thus, VNC neuromodulatory neurons are well positioned to directly modulate VNC locomotor circuits.

Activation of VNC Serotonergic Neurons Slows Walking Speed

Previous studies showed that neuromodulatory systems can regulate walking but have not addressed the role of VNC neuromodulatory subpopulations. Using the intersectional genetic tools described above, we addressed whether neuromodulatory neurons in the VNC alone are sufficient to modulate walking behavior. We optogenetically activated these neurons and measured walking speed using the Flywalker behavioral assay [25]. We found that activation of serotonergic VNC populations, but not dopaminergic or octopaminergic/tyraminergic VNC subpopulations, significantly reduced the average speed at which animals walk (Figure 1H).

Based on these results, we focused the remainder of our analysis on VNC serotonergic neurons (5-HT^{VNC}). To validate the fidelity of our serotonergic Gal4 driver line and to rule out co-secretion of other neurotransmitters, we performed immunostaining for markers of serotoninergic (5-HT), dopaminergic (TH), octopaminergic/tyraminergic (Tdc2), glutamatergic (VGlut), cholinergic (ChAT), and GABAergic (GABA) neurons (Figure S1). These experiments demonstrate that the *Trh-Gal4* line drives expression in 5-HT-expressing neurons and that these neurons do not express any of the other neurotransmitters we surveyed, suggesting that they are primarily serotonergic.

We next characterized the effects on locomotor behavior of activating 5-HT^{VNC} neurons by studying animals freely walking within an arena [57, 58]. This approach allowed us to measure not only an animal's speed but also its walking frequency, angular velocity, and preferred position within the arena (Figures S2A–S2C). As with our initial experiments, activation of 5-HT^{VNC} neurons is sufficient to dramatically slow average walking speed in this paradigm (Figure 2A). Interestingly, activation of 5-HT^{VNC} neurons does not change the overall amount of time animals spend walking, suggesting that speed changes are not simply due to a decrease in overall activity but instead reveal a bias toward slower walking speeds (Figures S2D and S2F). Unlike a previous study showing that overexpressing the serotonin transporter in all neurons caused flies to move away from the edge of the arena [45], we see no effect on the distribution of animals within the arena when we limit activation to 5-HT^{VNC} neurons (Figure S2D). We also find that activation of 5-HT^{VNC} neurons decreases the absolute angular velocity of walking flies (Figure S2D). Thus, although these flies walk slower, they also walk straighter than control flies. This latter observation is unexpected, because straighter trajectories are usually correlated with faster walking speeds (Figure S2F).

Inhibition of 5-HT^{VNC} Neurons Increases Walking Speed

Although activation of 5-HT^{VNC} neurons causes flies to walk more slowly, gain-of-function experiments such as these cannot determine whether and in what situations these neurons are normally used to modulate walking speed. To begin to address this question, we expressed the inward rectifying potassium channel Kir2.1 to constitutively inactivate 5-HT^{VNC} neurons. Although neurons were inactivated throughout development and adulthood, we did not observe a change in the number or anatomy of 5-HT^{VNC} neurons, suggesting that their development is not significantly affected (Figures S2H and S2I).

Consistent with the activation phenotype, inhibition of 5-HT^{VNC} neurons causes animals to walk faster (Figure 2B). In fact, the shifts in velocity produced by either optogenetic activation or constitutive inhibition of 5-HT^{VNC} neurons mirror each other (Figure 2C). In addition, 5-HT^{VNC} inactivation causes animals to increase their angular velocity (Figures S2E and S2G) and increases the percentage of time that animals spend walking (Figure S2E). The reciprocal effects on speed from either activating or silencing 5-HT^{VNC} neurons suggest that serotonin release in the VNC has the capacity to modulate baseline walking speed.

5-HT^{VNC} Neurons Are Active in Walking Flies

The opposing effects on speed when 5-HT^{VNC} neurons are activated or inhibited suggest that the activity of these neurons will co-vary with walk-stop transitions and velocity changes during baseline walking. To test this prediction, we performed functional calcium imaging of 5-HT^{VNC} processes while flies walked on a spherical treadmill (Figure S3A) [59]. To obtain the most robust signal, we focused on fibers in the neck connective, which are likely derived from a subset of ascending 5-HT^{VNC} neurons that target the brain (Figures S3B–S3D).

Activity in these fibers is highly correlated with walking (Figures 2D and 2E). Fluorescent calcium signals from these cells rise dramatically at the onset of each walking bout (Figure 2F). These signals are much weaker when animals perform other motor behaviors, like proboscis extension or grooming (Figure S3E). These results suggest that at least a subset of 5-HT^{VNC} neurons
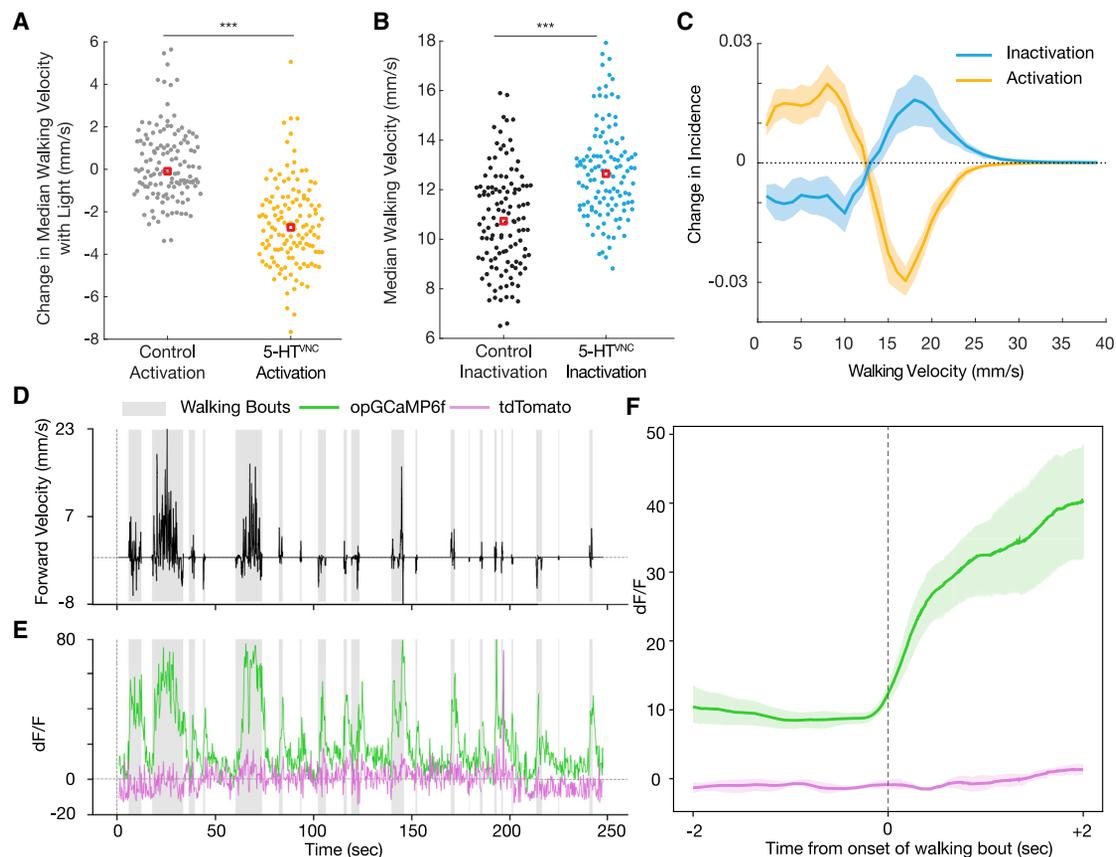
Figure 2. 5-HT^VNC Neurons Modulate Walking Speed

(A) Activation of 5-HT^VNC neurons (*Trh ∩ tsh > csChrimson* fed with ATR) causes animals to walk slower than background-matched non-Gal4 controls (*w^1118 ∩ tsh > csChrimson* fed with ATR). ***p < 0.001 by Kruskal-Wallis test. Red box indicates median. N = 130 animals for each genotype.

(B) Inactivation of 5-HT^VNC neurons (*Trh ∩ tsh > Kir2.1*) causes animals to walk faster than background-matched non-Gal4 controls (*w^1118 ∩ tsh > Kir2.1*). ***p < 0.001 by Kruskal-Wallis test. Red box indicates median. N = 119 animals per genotype.

(C) The distribution of velocity shifts caused by activation and inhibition of 5-HT^VNC neurons are symmetrical. Differences in population average histograms were calculated between control and experimental genotypes and were fit with 95% confidence intervals via bootstrapping. For activation experiments, behavior of *w^1118 ∩ tsh > csChrimson* flies fed with ATR was compared to that of *Trh ∩ tsh > csChrimson* flies also fed with ATR for the light on period only.

(D and E) Serotonergic processes passing through the cervical connective (labeled using *Trh ∩ tsh*) are active during walking. (D) A single animal's forward velocity with overlaid boxes showing defined walking bouts. (E) While tdTomato baseline signal (purple line) is not affected by walking bouts, the calcium signal (green line) in these serotonergic processes rises during walking bouts (gray boxes).

(F) Calcium signal but not tdTomato signal in these processes rises with the onset of walking bouts. For each animal, all walking bouts were synchronized around their onset, and an average was taken (between 80 and 130 walking bouts per animal). Plotted is the average of all animals (N = 5) with a 95% confidence interval representing the spread between animals.

See also Figures S2 and S3.

are specifically active when flies walk and are not generically active during all legged motor behaviors. We also find that the activity of these serotonergic processes positively correlates with the average speed of the walking bout, suggesting that these neurons may become more active when animals walk faster (Figure S3F).

The observation that the activity of some 5-HT^VNC neurons is positively correlated with velocity is interesting in light of our behavioral data, which show that flies walk more slowly when 5-HT^VNC neurons are optogenetically activated. There are several explanations for these apparently opposing observations. First, because the calcium imaging experiments only focus on a subset of 5-HT^VNC processes, while the behavior experiments manipulate the entire set of 5-HT^VNC neurons, it may be

that the neurons being imaged have a unique function and that their activity is not representative of the entire set. Alternatively, if their activity is representative of the broader population of 5-HT^VNC neurons, it would suggest that as flies walk faster more serotonin release is needed to slow animals down. Regardless, the fact that activity in these neurons correlates with velocity supports a role for them in modulating walking speed and raises the possibility that some of them may function in a negative feedback loop.

5-HT^VNC Activation Does Not Disrupt Walking Coordination

The slower walking speeds that result when 5-HT^VNC neurons are activated could be the result of poor coordination or,

alternatively, controlled adjustments of kinematic parameters, which naturally occur when flies walk more slowly [10, 25]. To distinguish between these two possibilities, we returned to the Flywalker assay, which measures kinematic parameters at high temporal and spatial resolution [25] (Figure S4A).

Using this assay, we find that optogenetic activation of 5-HT^{VNC} neurons results in highly coordinated walking patterns. Representative traces of an individual's footprints during a slow walking bout show that activation of these neurons does not perturb stereotyped foot placement or interfere with the straightness of the walking bout (Figures 3A and 3C). Step and stance traces show that these animals also use highly coordinated gaits, suggesting that interleg coordination is intact (Figures 3B and 3D). In fact, compared to control flies, 5-HT^{VNC} neuron activation results in more precise foot placement at the onset and offset of each stance phase, suggesting that the walking behavior of these animals is more constrained compared to control animals (Figure S4B).

In wild-type flies, most walking parameters are highly correlated with speed, shifting as animals walk faster or slower [10, 25]. For example, as animals walk slower, their step-cycle frequency decreases, they take longer steps, and they slow the velocity of their swinging legs. These shifts are accompanied by a shift in the step duty cycle, as stance duration increases while swing duration remains largely unchanged [10, 25]. When 5-HT^{VNC} neurons are activated, these relationships are maintained and extended into the slower speed range (Figures 3E–3I). Similarly, as animals walk more slowly, their preferred gait shifts from the three-legged tripod gait to more stable tetrapod and wave gaits [10, 25]. Upon activation of 5-HT^{VNC} neurons, animals continue the trend to preferentially use these slower walking gaits (Figures 3J–3L). In some cases, such as step length (Figure 3G) and stance duration (Figure 3I), the parameter-speed relationship when 5-HT^{VNC} neurons are activated is an extrapolation of the wild-type relationship, while, in other cases, such as the choice of tripod gait (Figure 3J), the relationship with speed is altered when these neurons are activated. Most of the other parameters fall in between these two extremes.

5-HT^{VNC} Neuron Inactivation Slows Walking in Multiple Contexts

Results from our behavioral experiments suggest a model whereby the VNC serotonergic system is used to regulate walking speed: when the system is activated, flies walk more slowly and when the system is silenced, flies walk faster. Based on these observations, we next tested whether this system is required for flies to naturally adjust their baseline walking speeds. To test this hypothesis, we silenced 5-HT^{VNC} neurons under conditions when flies normally walk at different speeds, including multiple temperatures, body orientations, nutritional states, and in response to mechanosensory stimulation [3, 53, 60–62]. Counter to our expectation, animals in which 5-HT^{VNC} neurons were silenced are still able to adjust their speed in the same direction as wild-type flies in all of these contexts (Figure 4A). For example, compared to 25°, flies walk slower at 18°C and faster at 30°C even when 5-HT^{VNC} neurons are silenced, arguing that this system is not required for flies to modulate their speed in response to this difference. In addition, these data reveal that, for all of the contexts tested here, animals

in which 5-HT^{VNC} neurons are silenced walk faster than their matched controls. For example, 5-HT^{VNC}-silenced flies walk faster at 18°C compared to control flies at 18°C. Thus, we further conclude that serotonin release in the VNC slows walking speed across a wide spectrum of environmental contexts. These findings are consistent with a model where the VNC serotonergic system acts as a mild and constitutive break on walking speed, independently of how fast or slow this speed is set by other mechanisms. However, we note that because we are using constitutive inactivation tools, we cannot currently rule out that the observed phenotypes are in part the result of compensation within the network when 5-HT^{VNC} neurons are silenced.

Silencing 5-HT^{VNC} Neurons Alters the Response to Sudden Changes in the Environment

Although the above results suggest the VNC serotonergic system is not needed for flies to adjust their baseline walking speed in many situations, another potentially valuable role for slowing walking speed might be as a response to when animals are startled. In mammals, stereotyped startle behaviors occur in response to a wide variety of sensory stimuli—acoustic, tactile, and vestibular. These responses take place on sub-second timescales, involve simultaneous contraction of muscles throughout the body, and are similar irrespective of the initiating stimulus [63, 64]. Like mammals, *Drosophila* display stereotyped responses to threatening looming stimuli, beginning with an initial freezing period lasting less than a second before escape behaviors are initiated [65–67]. Because these startle responses are contextually independent and have been shown to be mediated in part by serotonin in mammals [68], we asked whether 5-HT^{VNC} neurons are required for these responses in *Drosophila*.

We tested this idea using two different startle-inducing paradigms: (1) one in which flies abruptly experience total darkness ("blackout paradigm") and (2) one in which flies suddenly experience strong mechanical stimulation, such as an intense vibration ("earthquake paradigm") [61]. In both scenarios, control animals on average show a two-tiered response to these abrupt changes (Figures 4B and 4C): first, many animals rapidly come to a nearly complete stop and then they pause before resuming a behavior that is appropriate for the new context (schematized in Figure 4D). For both the blackout and earthquake paradigms, on average control animals stop within the first 0.25 s, pause for about a second, and then resume walking (Figures 4B and 4C). Animals lacking the ability to release serotonin in the VNC are deficient in these initial responses (Figures 4B, 4C, 4E, and 4F) but still eventually achieve context-appropriate walking speeds (Figure 4A). Moreover, consistent with our earlier analyses, flies with silenced 5-HT^{VNC} neurons walk faster compared to control flies, both before and after the startle-inducing stimulus (Figures 4B and 4C).

Thus, in addition to serving as a constitutive break on locomotor speed, these results suggest that the serotonergic system helps to facilitate an immediate and stimulus-independent pause response when flies are startled.

Different Serotonin Receptor Mutants Alter the Startle Response in Different Ways

All five serotonergic receptors in *Drosophila*—5-HT1A, 5-HT1B, 5-HT2A, 5-HT2B, and 5-HT7—are G-protein-coupled receptors
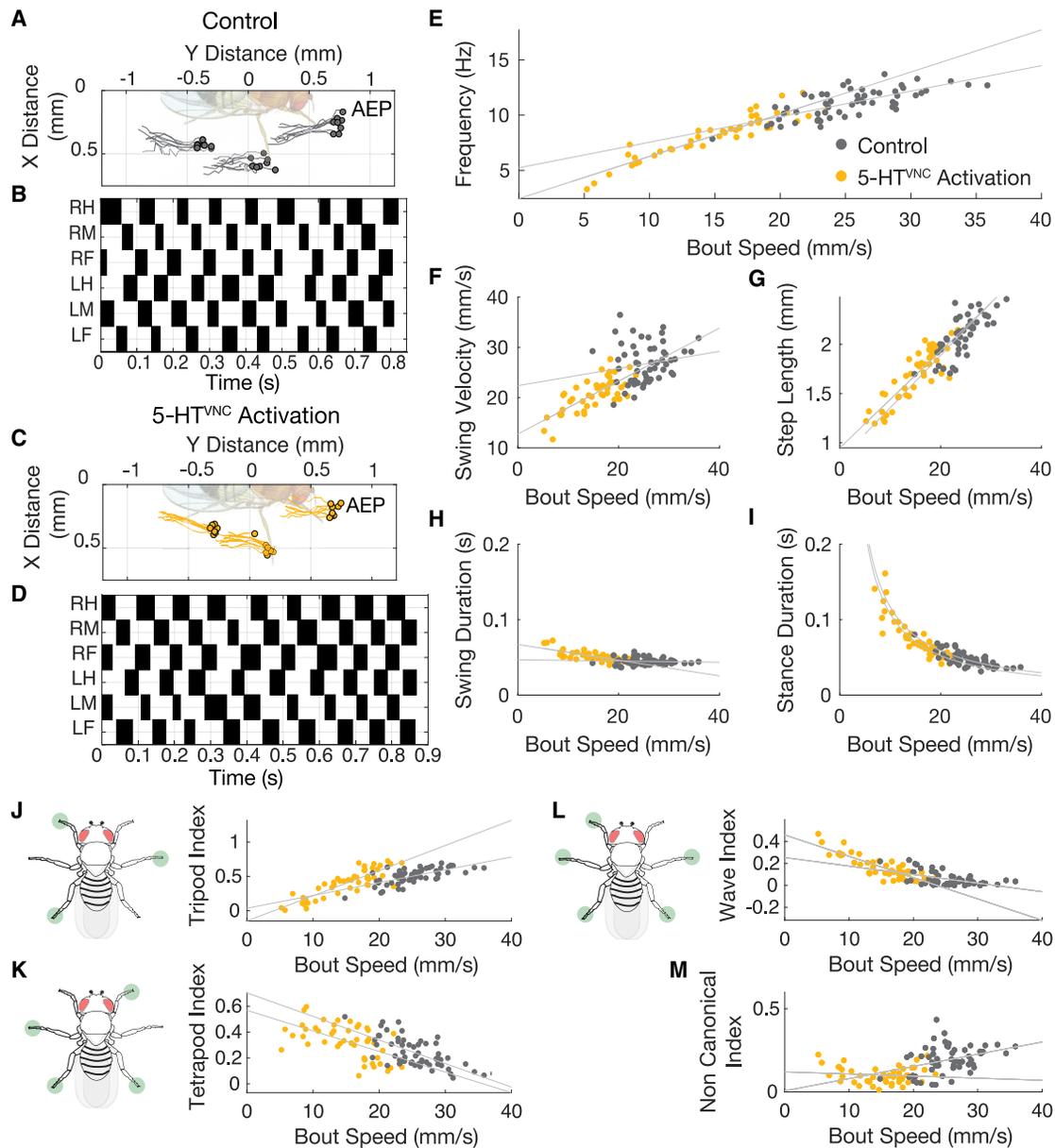
Figure 3. Walking Is Coordinated When 5-HT^{VNC} Neurons Are Activated

(A–D) Representative data from speed-matched slow (19 mm/s) walking bouts show that activation of 5-HT^{VNC} neurons does not disrupt locomotor coordination. Footfalls (filled circles) and stance traces (lines) for all steps taken by the left front, middle, and hind legs show foot touchdown placement is consistent over time and stance traces are relatively straight in both control animals (*Trh ∩ tsh > csChrimson* grown on food lacking ATR) (A) and animals where 5-HT^{VNC} neurons have been activated (*Trh ∩ tsh > csChrimson* fed with ATR) (C). Step trace for each leg during a walking bout for control (B) and experimental (D) animals. Stance phase is indicated in white and swing phase in black. The checkerboard pattern is consistent with a highly coordinated walking gait.

(E–I) Quantification of step parameters upon activation of 5-HT^{VNC} neurons. The relationships between speed and frequency (E), swing velocity (F), step length (G), swing duration (H), and stance duration (I) extend the trends observed with control flies. n = 47 bouts from N = 10–23 animals for *Trh ∩ tsh > csChrimson* ATR$^+$ (yellow circles). n = 56 bouts from N = 12–30 animals for *Trh ∩ tsh > csChrimson* ATR$^-$ (gray circles). Speed by ATR interaction effect in multivariable model: frequency ($p < 0.001$), swing velocity ($p = 0.02$), step length ($p = 0.53$), swing duration ($p < 0.001$), and stance duration ($p = 0.71$).

(J–M) Quantification of gait selection upon activation of 5-HT^{VNC} neurons. Activation of 5-HT^{VNC} neurons increases wave (L) and tetrapod (K) gait utilization while decreasing time spent using tripod (J) gait. There is a low frequency of non-canonical gait conformations upon activation (M). n = 47 bouts from N = 10–23 animals for *Trh ∩ tsh > csChrimson* ATR$^+$ (yellow circles). n = 56 bouts from N = 12–30 animals for *Trh ∩ tsh > csChrimson* ATR$^-$ (gray circles). Speed by ATR interaction effect in multivariable model: tripod index ($p < 0.001$), tetrapod index ($p = 0.60$), wave index ($p < 0.001$), and non-canonical ($p = 0.006$).
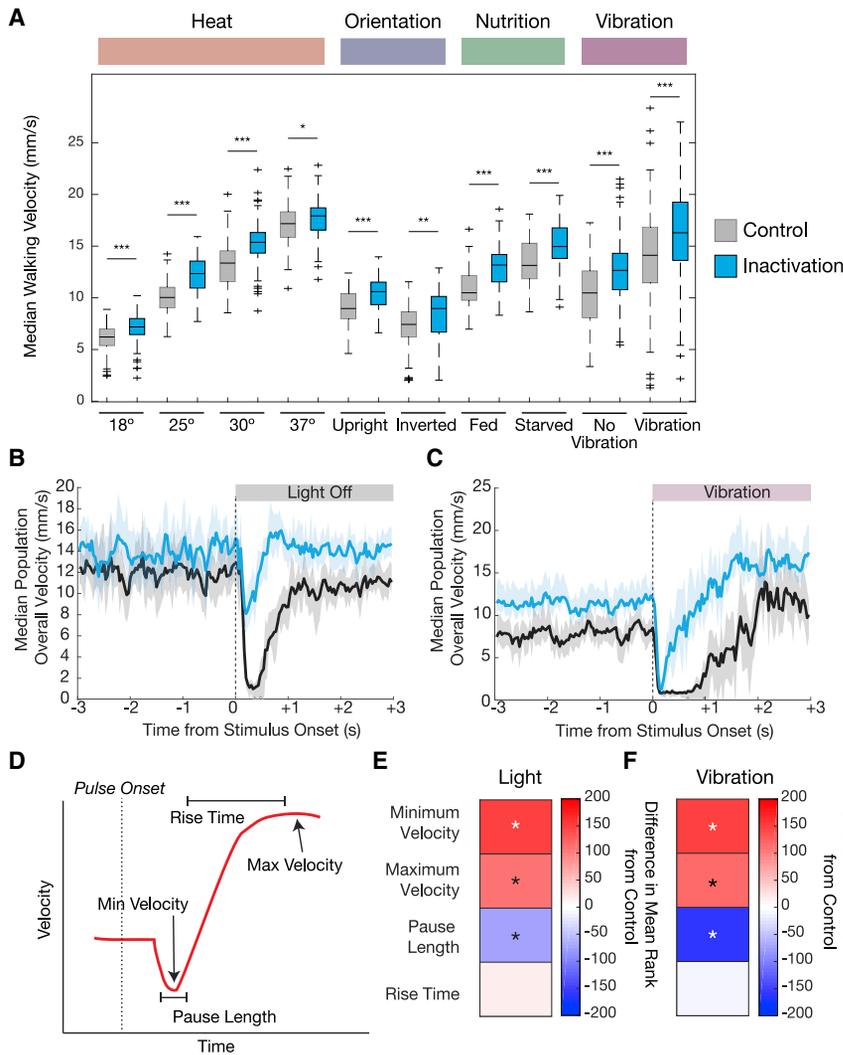
See also Figure S4.

Figure 4. Changes in Walking Behavior When 5-HT^{VNC} Neurons Are Silenced

(A) Silencing 5-HT^{VNC} neurons (*Trh* ∩ *tsh* > *Kir2.1*) causes an increase in walking speed compared to genetically background-matched non-Gal4 controls (*w^{1118}* ∩ *tsh* > *Kir2.1*) across a diversity of behavioral contexts including different temperatures, orientations, nutritional states, and vibration stimuli. For each condition, genotypes were compared using a Kruskal-Wallis test, ***p < 0.001, **p < 0.01, *p < 0.05 by Kruskal-Wallis test. For all conditions, p < 0.001 for context effects for both control and experimental genotypes; 18°C, N = 130 per genotype; 25°C, N = 120 per genotype; 30°C, N = 120 per genotype; 37°C, N = *w^{1118}* (120) *Trh* (119); upright, N = 90 per genotype; inverted *w^{1118}* (74) *Trh* (70); fed, N = 86 per genotype; starved, N = *w^{1118}* (86) *Trh* (85); vibration, N = *w^{1118}* (165) *Trh* (164).

(B and C) Silencing 5-HT^{VNC} neurons changes the immediate behavioral responses to sudden contextual changes. When lights switch from on to off (B), control animals (*w^{1118}* ∩ *tsh* > *Kir2.1*, shown in black) show a brief behavioral pause and then resume activity. When 5-HT^{VNC} neurons are silenced (*Trh* ∩ *tsh* > *Kir2.1*, shown in blue), animals still slow their speed but do not fully pause. In response to the onset of vibration (C) control animals stop, pause, and then accelerate speed. When 5-HT^{VNC} neurons are silenced (*Trh* ∩ *tsh* > *Kir2.1*, shown in blue), animals pause but re-accelerate more quickly than controls. Shaded areas show 95% confidence intervals. For light experiments, N = *w^{1118}* (150) *Trh* (140); for vibration experiments N = *w^{1118}* (167) *Trh* (166).

(D) Schematic of behaviors in response to a sudden stimulus. This response is divided into four key parameters that describe different phases of the response, indicated with arrows and bounded lines.

(E and F) Heatmaps quantifying the parameters schematized in (D) when 5-HT^{VNC} neurons are inactivated in response to the blackout (E) and

earthquake (F) scenarios. Plotted for every genotype is the difference in mean ranks (Kruskal-Wallis test statistics) for each parameter compared to *w^{1118}* ∩ *tsh* > *Kir2.1* control flies. Starred parameters are those where differences between control and experimental animals consistently reached significance (p < 0.05; see STAR Methods).

See also Figure S5.

(GPCRs) [69, 70]. Like their mammalian orthologs, members of each serotonin receptor family (1, 2, and 7) have distinct effects upon activation. Receptors in the 1 family, 5-HT1A and 5-HT1B, act through the G$_i$ pathway to inhibit the generation of cAMP, whereas 5-HT7, the only member of the 7 family in *Drosophila*, stimulates the production of cAMP [71, 72]. Receptors of the 2 family, 5-HT2A and 5-HT2B in *Drosophila*, act through the PLC-IP$_3$ signaling pathway to increase intracellular calcium [70, 73, 74]. Together, this diversity of receptors is thought to allow serotonin to produce complex physiological responses that depend on both synaptic connectivity and receptor expression patterns.

Before characterizing the phenotypes of these receptor mutants, we analyzed a mutant of the *Trh* gene (*Trh^{01}*), which is globally unable to produce serotonin [47]. Reassuringly, *Trh^{01}* animals show a similar phenotype to animals in which 5-HT^{VNC} neurons were silenced: flies walk significantly faster and more frequently than controls and exhibit a similar startle response in the earthquake paradigm (Figures 5A, 5B, and 5G). In addition, *Trh^{01}* mutant animals walk closer to the edge of the arena compared to control animals, consistent with previous observations [45] (Figure S5A).

Null receptor mutants *5-HT1A^{Gal4}*, *1B^{Gal4}*, *2A^{Gal4}*, and *7^{Gal4}* all increase the percentage of time animals spend walking (Figure S5A) [47]. However, an increase in walking speed is only observed in *5-HT7^{Gal4}* mutants (Figure 5A), suggesting that 5-HT7 is the primary receptor responsible for mediating the effects of serotonin on walking speed.

We next tested the receptor mutants in the earthquake paradigm. Interestingly, *5-HT7^{Gal4}* and *5-HT1B^{Gal4}* mutants closely phenocopy the startle response seen in *Trh^{01}* mutants and also in the 5-HT^{VNC} inactivation experiments (Figures 5C, 5D, and 5G; Figures S5C–S5E). By contrast, although *5-HT1A^{Gal4}* and *5-HT2A^{Gal4}* mutants do not show a dramatic change in pause
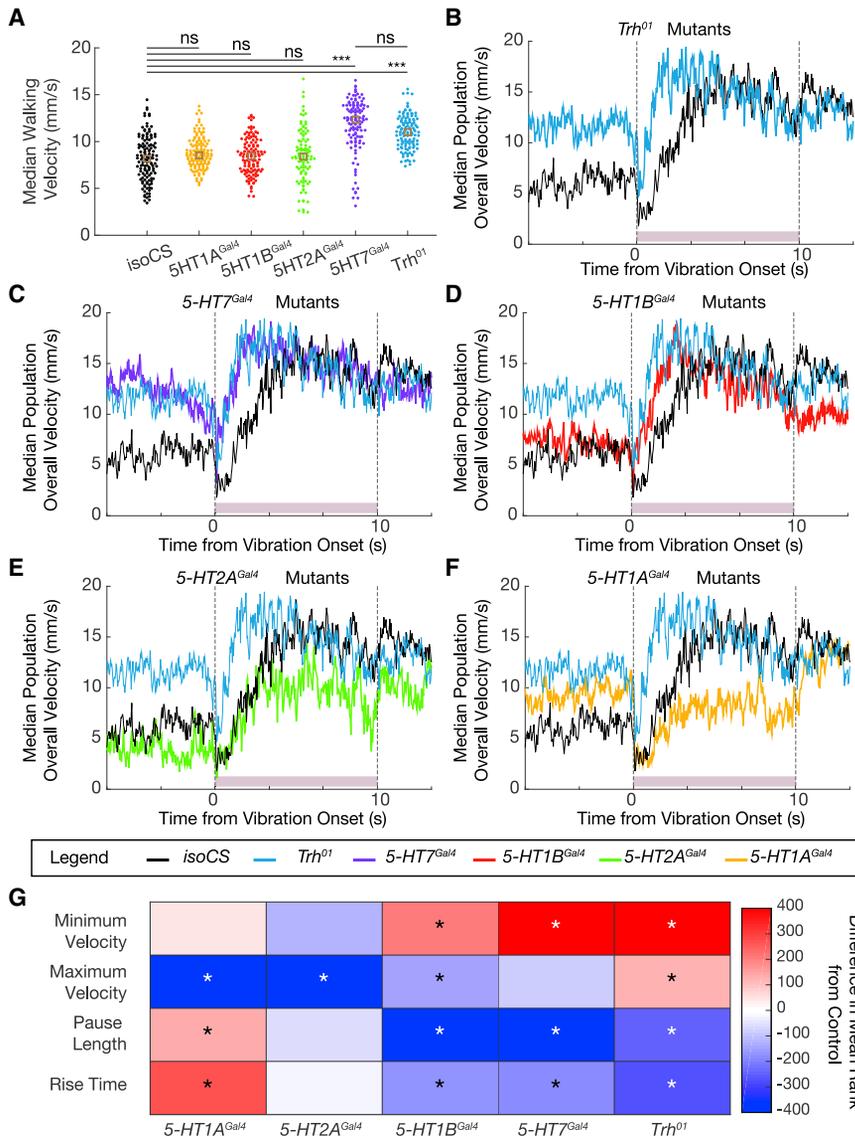
Figure 5. Phenotype of the Startle Response of *Trh* and Serotonin Receptor Mutants

(A) Dot plot showing median population walking speed during a 5-min recording session for *Trh01* mutants (blue), which walk faster than background-matched *isoCS* controls (black), consistent with the 5-HT^VNC inactivation experiments. *5-HT7Gal4* mutants (purple) also walk faster than controls, but the other receptor mutants do not. ***p < 0.001, **p < 0.01, *p < 0.05 ns p > 0.05 by Kruskal-Wallis analysis with Dunn-Sidak correction for multiple comparisons. Brown box indicates median. N = *isoCS* (130) *5-HT1AGal4* (130) *5-HT1BGal4* (120) *5-HT2AGal4* (100) *5-HT7Gal4* (120) *Trh01* (120).

(B–F) Median population walking speed sampled at 30 Hz in response to vibration stimulus. *Trh01* mutants (B, blue line) show a blunted and shortened pause in response to the novel stimulus. *5-HT7Gal4* mutants (C, purple line) and *5-HT1BGal4* mutants (D, red line) show a similar phenotype to *Trh01* mutants. *5-HT2AGal4* mutants (E, green line) and *5-HT1AGal4* mutants (F, yellow line) have a pause phase comparable to controls, but do not accelerate as much in response to the vibration stimulus. N = *isoCS* (140) *5-HT1AGal4* (115) *5-HT1BGal4* (124) *5-HT2AGal4* (88) *5-HT7Gal4* (120) *Trh01* (139)

(G) Heatmap showing how lack of *Trh* or serotonergic receptors affects the response to vibration stimulus. Plotted for every genotype is the difference in mean ranks (Kruskal-Wallis test with Dunn-Sidak correction for multiple comparisons statistics) for each parameter compared to *isoCS* control flies. Starred parameters are those where differences between control and experimentals consistently reached significance (p < 0.05, see STAR Methods).

See also Figure S5.

---

length, they exhibit a sustained decrease in their final target speed in response to this stimulus (Figures 5E–5G; Figures S5F and S5G).

These data are consistent with the idea that different receptors influence distinct aspects of the startle response. Notably, mutation of receptors that are predicted to have opposing effects on cAMP production, such as 5-HT1B and 5-HT7, can result in similar phenotypes. Further, some receptor mutants exhibit phenotypes that are not seen in *Trh01* mutant animals. These complex changes in locomotor behavior might be explained by the differential expression of serotonin receptors in key components of the locomotor circuit.

Serotonin Receptors Are Expressed in Distinct Cell Types

The different effects on walking observed in flies mutant for different serotonin receptors suggest that, in addition to

distinct biochemical properties, they may also have different expression patterns within the locomotor circuit. To identify neurons that express these receptors, we used gene and protein trap Gal4 lines from the MiMIC library to drive expression of a GFP reporter in the pattern of each receptor subtype [75] (Figure S6G). Each receptor line drives expression in many neurons both within the brain and the VNC (Figures 6A–6E). Many of these are uncharacterized interneurons that cannot yet be functionally studied. However, each serotonin receptor is also expressed in distinct subsets of leg motor and sensory neurons. In particular, while members of the 5-HT1 family are predominantly expressed in mechanosensory neurons throughout the legs, 5-HT2 and 5-HT7 receptors are expressed in proximal-targeting flexor and extensor motor neurons (Figures S6A–S6F), proprioceptive, and distal sensory neuron populations (Figures 6F–6K). Thus, serotonin release in the VNC is likely to differentially affect these components of the locomotor circuit, which we
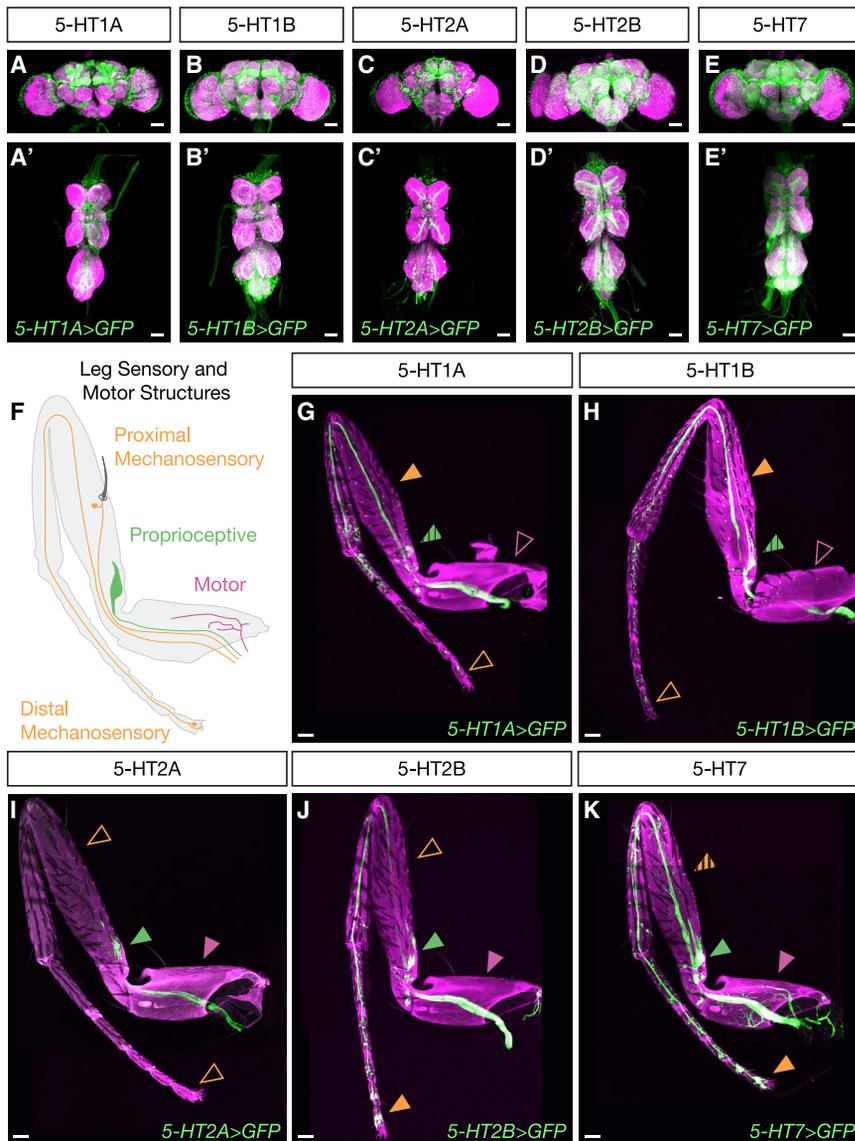
Figure 6. Differential Expression of Serotonin Receptors in Locomotor Circuit Components

(A–E) Maximum intensity projections show Gal4-driven expression of serotonin receptors in both the brain (A–E) and VNC (A'–E'). All scale bars are 50 μm.

(F) Schematic of sensory and motor neuron populations in an adult leg.

(G–K) Maximum intensity projections show Gal4-driven expression of serotonin receptors in neuronal processes in the adult leg. Each receptor is expressed in a distinct pattern in sensory-motor components. While some are expressed in motor neurons (purple arrows, hatched arrows indicate limited or weak expression) and proprioceptive neurons (green arrows), others are not. All receptors are expressed in a subset of mechanosensory neurons (orange arrows), but some are preferentially expressed in proximal or distal leg segments. All scale bars are 50 μm.

See also Figure S6.

A Common Role for Serotonin in Modulating Walking Speed across Species

A central finding of our study is that serotonergic neuron activity in the VNC modulates baseline walking speed in *Drosophila*. This finding parallels previous observations in the motor systems of other organisms. For example, consistent with our calcium imaging experiments, activity of serotonergic neurons in the cat brainstem is correlated with motor behavior and walking speed [76, 77]. Additionally, in vertebrates as diverse as the lamprey and cat, serotonin induces an increase in oscillatory and step-cycle period, respectively, slowing locomotion [40, 41]. One recent study in mice showed that activation of the dorsal raphe nucleus—a key serotonergic brain region—produces rapid suppression of spontaneous locomotion and locomotor speed, while showing minimal effect on kinematic parameters, such as gait, or on non-locomotor behaviors such as grooming [78]. Although this study focused on a subset of serotoninergic neurons targeting the forebrain, the parallels to our results suggest that the modulatory role of the serotonergic system in regulating locomotor speed is remarkably conserved across the animal kingdom.

Serotonergic Modulation of the Startle Response

In our experiments, we observed that the onset of a startling stimulus (be it visual or mechanosensory) induces a brief period of pausing behavior in wild-type flies. We hypothesize that these behavioral pauses are similar to startle responses seen in both mammalian systems and some species of insects, which also have a pause phase before animals embark on an

hypothesize ultimately contributes to the observed changes in behavior.

DISCUSSION

Walking is a highly stereotyped behavior, consisting of a small number of well-defined gaits, each with its own set of characteristic kinematic parameters. However, walking must also be flexible, to adapt to a wide variety of environments, complex terrains, and novel situations. How nervous systems manage to orchestrate behaviors that are simultaneously stereotyped and flexible is not well understood. Here, we show in the fly that (1) serotonergic VNC neural activity can modulate walking speed in a wide variety of contexts and (2) these neurons play a role in a fly's response to the sudden onset of a startling stimulus. Below, we discuss these findings and present a preliminary model that summarizes serotonin's role in modulating walking behavior.

appropriate behavioral action [63, 64, 66–68, 79, 80]. In *Drosophila* and the locust, these pauses are thought to optimally prepare animals for maximally effective escape behaviors. For example, prior to initiating flight in response to a looming threat, *Drosophila* pause for about 200 ms to execute a series of postural adjustments that help orient the direction of takeoff [67]. It may also be that pauses allow animals to collect additional sensory information before they select an appropriate response to the startling stimulus. Interestingly, however, not all insects appear to exhibit a pause phase; for example, studies of the American cockroach, *Periplaneta americana*, suggest that the escape behavior in response to a predator is immediate [81].

Although our $5HT^{VNC}$ silencing experiments were done using constitutive inactivation tools, which makes it difficult to rule out a developmental defect, the similar phenotype exhibited by the *Trh* mutant argues that the inability to release serotonin from these neurons is the cause of the startle response defect. In mammals, the absence of serotonin, due to the lesion of key serotonergic brain regions or pharmacological blockade, is generally associated with an increase in the intensity of startle responses [82, 83]. Although this may seem counter to our results, other studies have shown that serotonin increases startle responses when injected directly into the lumbar spinal cord [84, 85]. Thus, serotonin may play distinct roles in the forebrain and in the spinal cord. Together with our results, we suggest that the role of spinal cord/VNC serotonin release is to extend the duration of and/or amplify the startle response.

A Model for Serotonin-Mediated Modulation of Walking in Flies

Putting the various lines of evidence presented here together, we can formulate a preliminary model for serotonin's role in modulating *Drosophila* walking behavior. First, we suggest that one function of serotonin release in the VNC is to act as a mild constitutive brake. In non-startle contexts, the system would oppose forward acceleration that is driven by other inputs, such as descending commands from the brain [4, 17, 86]. Consistent with this idea, when the brake is removed ($5-HT^{VNC}$ neurons are silenced), flies walk slightly faster, and, when the brake is stronger ($5-HT^{VNC}$ neurons are activated), flies slow down. The calcium imaging results showing that the activity of a subset of $5-HT^{VNC}$ neurons increases as flies walk faster suggest that the brake may be stronger at higher speeds. A caveat to this latter idea is that the calcium imaging experiments monitored only a subset of the $5-HT^{VNC}$ neurons, raising the possibility that the activity of other $5-HT^{VNC}$ neurons have a different relationship with speed.

When flies are startled, our data are consistent with the idea that serotonin release in the VNC serves to put a strong brake on walking speed, presumably to allow flies to prepare for an appropriate behavioral response. When the $5-HT^{VNC}$ neurons are silenced, flies are unable to apply this brake and consequently have a compromised response. Notably, however, even when these neurons are silenced flies are still able to respond, albeit more weakly, to being startled, suggesting that part of the response is still intact. One possibility is that, in addition to triggering a serotonin-mediated brake, the response to

being startled may also independently dampen the accelerator, reducing walking drive.

The observation that serotonin release in the VNC similarly affects the response to both the earthquake and blackout paradigms, which are perceived by two very different sensory systems, suggests that this neuromodulator is affecting locomotor components that are shared by both systems. Although the expression of 5-HT receptors in sensory and motor neurons is consistent with this notion, we note that this model is likely incomplete as we cannot as of now incorporate the role of local interneurons that also express 5-HT receptors.

Nevertheless, because the primary receptors expressed in motor neurons are 5-HT7 and 5-HT2B, which have been shown to upregulate the production of cAMP and facilitate calcium entry [70], we hypothesize that serotonin amplifies activity in these motor neurons. There is ample evidence in the literature to support this role for serotonin both in rodent models as well as in human studies [87, 88]. Further, the motor neurons expressing these serotonergic receptors target both flexor and extensor muscles in the coxa and femur, two proximal leg segments. These observations suggest that serotonin acting on these motor neurons may facilitate co-contraction, a mechanism that would partially stiffen these leg joints, potentially resulting in slower walking speeds. Consistent with this notion, co-contraction has been shown to enable joint stability in the face of a complex environment and also during the preparatory phase for certain escape behaviors [67, 80, 89–91]. Co-contraction of tibia flexor and extensor muscles is also part of the initial pause phase of the startle response in the locust, suggesting that this mechanism may be shared [80].

In addition to motor neurons, serotonin receptors are expressed in distinct classes of leg sensory neurons that target the leg neuropils of the VNC. Considering the broad expression of serotonergic receptors in sensory organs, it is interesting that one of the behavioral roles of serotonin we identified is its ability to mediate the response to vibration. Vibration is sensed by the chordotonal organ, and our expression analysis reveals that serotonin receptors are expressed to different extents in chordotonal neurons [24, 92, 93]. Together, these observations suggest that modulation of sensory information as it is entering the VNC could play a key role in how serotonin modulates the response to a vibration stimulus.

Finally, the observed distribution of serotonergic receptor subtypes in sensory processes may serve to shift the balance of sensory information as a consequence of serotonergic input. Based on the known downstream signaling properties of these receptors, we predict that increased levels of serotonin in the VNC would amplify proprioceptive and distal sensory inputs at the expense of more proximal sensory information. These shifts in sensory processing may also contribute to increased stability and might be useful in other contexts where slow walking is preferred, such as navigating complex terrains where improved sensory information might be beneficial. It may also be that these shifts in sensory input are important during the pause phase of the startle response, as they may allow animals to gather valuable information in order to compute the next phase of escape behaviors.

CellPress

STAR★METHODS

Detailed methods are provided in the online version of this paper and include the following:

- KEY RESOURCES TABLE
- LEAD CONTACT AND MATERIAL AVAILABILITY
- EXPERIMENTAL MODEL AND SUBJECT DETAILS
  - Fly Husbandry
  - Fly Genotypes with Associated Figures
- METHOD DETAILS
  - Immunostaining Brain and VNC
  - Confocal Imaging of Brains and VNCs
  - Cell Counting and Quantification
  - Leg Dissection, Imaging, and Image Processing
  - Arena Experiments
  - Flywalker Experiments
  - Functional Imaging Experiments
- QUANTIFICATION AND STATISTICAL ANALYSIS
  - Arena Experiments
  - Flywalker Experiments
  - Functional Imaging Experiments
- DATA AND CODE AVAILABILITY

SUPPLEMENTAL INFORMATION

Supplemental Information can be found online at https://doi.org/10.1016/j.cub.2019.10.042.

AUTHOR CONTRIBUTIONS

C.E.H. and R.S.M. conceived of the project and designed the experiments; T.T. and R.H. designed and built the behavior rigs; C.E.H. conducted all of the experiments and performed all data analysis, with the exception of calcium imaging experiments, which were carried out by C.-L.C. and analyzed by C.E.H., C.-L.C., and P.R.; C.E.H. and R.S.M. wrote the paper, and P.R. edited it.

DECLARATION OF INTERESTS

The authors declare no competing interests.

REFERENCES

1. Ritzmann, R.E., and Büschges, A. (2007). Adaptive motor behavior in insects. Curr. Opin. Neurobiol. *17*, 629–636.

2. Ritzmann, R.E., Quinn, R.D., and Fischer, M.S. (2004). Convergent evolution and locomotion through complex terrain by insects, vertebrates and robots. Arthropod Struct. Dev. *33*, 361–379.

3. Mendes, C.S., Rajendren, S.V., Bartos, I., Márka, S., and Mann, R.S. (2014). Kinematic responses to changes in walking orientation and gravitational load in Drosophila melanogaster. PLoS ONE *9*, e109204.

4. Bidaye, S.S., Machacek, C., Wu, Y., and Dickson, B.J. (2014). Neuronal control of Drosophila walking direction. Science *344*, 97–101.

5. Isakov, A., Buchanan, S.M., Sullivan, B., Ramachandran, A., Chapman, J.K.S., Lu, E.S., Mahadevan, L., and de Bivort, B. (2016). Recovery of locomotion after injury in Drosophila melanogaster depends on proprioception. J. Exp. Biol. *219*, 1760–1771.

6. Pick, S., and Strauss, R. (2005). Goal-driven behavioral adaptations in gap-climbing Drosophila. Curr. Biol. *15*, 1473–1478.

7. Blaesing, B., and Cruse, H. (2004). Stick insect locomotion in a complex environment: climbing over large gaps. J. Exp. Biol. *207*, 1273–1286.

8. Strauss, R., and Heisenberg, M. (1990). Coordination of legs during straight walking and turning in Drosophila melanogaster. J. Comp. Physiol. A Neuroethol. Sens. Neural Behav. Physiol. *167*, 403–412.

9. Couzin-Fuchs, E., Kiemel, T., Gal, O., Ayali, A., and Holmes, P. (2015). Intersegmental coupling and recovery from perturbations in freely running cockroaches. J. Exp. Biol. *218*, 285–297.

10. Wosnitza, A., Bockemühl, T., Dübbert, M., Scholz, H., and Büschges, A. (2013). Inter-leg coordination in the control of walking speed in Drosophila. J. Exp. Biol. *216*, 480–491.

11. Pearson, K.G. (1993). Common principles of motor control in vertebrates and invertebrates. Annu. Rev. Neurosci. *16*, 265–297.

12. Harris-Warrick, R.M., and Marder, E. (1991). Modulation of neural networks for behavior. Annu. Rev. Neurosci. *14*, 39–57.

13. Graham, D. (1985). Pattern and Control of Walking in Insects. In Advances in Insect Physiology Advances in Insect Physiology, M.J. Berridge, J.E. Treherne, and V.B. Wigglesworth, eds. (Academic Press), pp. 31–140.

14. Court, R.C., Armstrong, J.D., Borner, J., Card, G., Costa, M., Dickinson, M., Duch, C., Korff, W., Mann, R., Merritt, D., et al. (2017). A Systematic Nomenclature for the Drosophila Ventral Nervous System. bioRxiv. https://doi.org/10.1101/122952.

15. Venkatasubramanian, L., and Mann, R.S. (2019). The development and assembly of the Drosophila adult ventral nerve cord. Curr. Opin. Neurobiol. *56*, 135–143.

16. Truman, J.W., Schuppe, H., Shepherd, D., and Williams, D.W. (2004). Developmental architecture of adult-specific lineages in the ventral CNS of Drosophila. Development *131*, 5167–5184.

17. Namiki, S., Dickinson, M.H., Wong, A.M., Korff, W., and Card, G.M. (2018). The functional organization of descending sensory-motor pathways in *Drosophila*. eLife *7*. Published online June 26, 2018. https://doi.org/10.7554/eLife.34272.

18. Baek, M., and Mann, R.S. (2009). Lineage and birth date specify motor neuron targeting and dendritic architecture in adult Drosophila. J. Neurosci. *29*, 6904–6916.

19. Brierley, D.J., Blanc, E., Reddy, O.V., Vijayraghavan, K., and Williams, D.W. (2009). Dendritic targeting in the leg neuropil of Drosophila: the role of midline signalling molecules in generating a myotopic map. PLoS Biol. Published online September 22, 2009. https://doi.org/10.1371/journal.pbio.1000199.

20. Tuthill, J.C., and Azim, E. (2018). Proprioception. Curr. Biol. *28*, R194–R203.

21. Murphey, R.K., Possidente, D.R., Vandervorst, P., and Ghysen, A. (1989). Compartments and the topography of leg afferent projections in Drosophila. J. Neurosci. *9*, 3209–3217.

22. Tuthill, J.C., and Wilson, R.I. (2016). Mechanosensation and Adaptive Motor Control in Insects. Curr. Biol. *26*, R1022–R1038.

23. Büschges, A. (2005). Sensory control and organization of neural networks mediating coordination of multisegmental organs for locomotion. J. Neurophysiol. *93*, 1127–1135.

24. Field, L., and Matheson, T. (1998). Chordotonal Organs of Insects. Adv. Insect Physiol. *27*, 1–228.

25. Mendes, C.S., Bartos, I., Akay, T., Márka, S., and Mann, R.S. (2013). Quantification of gait parameters in freely walking wild type and sensory deprived Drosophila melanogaster. eLife. Published online January 8, 2013. https://doi.org/10.7554/eLife.00231.

26. Yellman, C., Tao, H., He, B., and Hirsh, J. (1997). Conserved and sexually dimorphic behavioral responses to biogenic amines in decapitated Drosophila. Proc. Natl. Acad. Sci. USA *94*, 4131–4136.

27. Burrows, M. (1992). Local circuits for the control of leg movements in an insect. Trends Neurosci. *15*, 226–232.

28. Stein, W., Büschges, A., and Bässler, U. (2006). Intersegmental transfer of sensory signals in the stick insect leg muscle control system. J. Neurobiol. *66*, 1253–1269.

29. Büschges, A., and Manira, A.E. (1998). Sensory pathways and their modulation in the control of locomotion. Curr. Opin. Neurobiol. *8*, 733–739.

30. Pearson, K.G. (1995). Proprioceptive regulation of locomotion. Curr. Opin. Neurobiol. *5*, 786–791.

31. Grillner, S., and Zangger, P. (1979). On the central generation of locomotion in the low spinal cat. Exp. Brain Res. *34*, 241–261.

32. Bekoff, A., Nusbaum, M.P., Sabichi, A.L., and Clifford, M. (1987). Neural control of limb coordination. I. Comparison of hatching and walking motor output patterns in normal and deafferented chicks. J. Neurosci. *7*, 2320–2330.

33. Marder, E., and Bucher, D. (2001). Central pattern generators and the control of rhythmic movements. Curr. Biol. *11*, R986–R996.

34. Rossignol, S., Dubuc, R., and Gossard, J.-P. (2006). Dynamic sensorimotor interactions in locomotion. Physiol. Rev. *86*, 89–154.

35. Pearson, K.G. (2000). Neural adaptation in the generation of rhythmic behavior. Annu. Rev. Physiol. *62*, 723–753.

36. Marder, E. (2012). Neuromodulation of neuronal circuits: back to the future. Neuron *76*, 1–11.

37. Dickinson, P.S. (2006). Neuromodulation of central pattern generators in invertebrates and vertebrates. Curr. Opin. Neurobiol. *16*, 604–614.

38. Harris-Warrick, R.M. (2011). Neuromodulation and flexibility in Central Pattern Generator networks. Curr. Opin. Neurobiol. *21*, 685–692.

39. Morton, D.W., and Chiel, H.J. (1994). Neural architectures for adaptive behavior. Trends Neurosci. *17*, 413–420.

40. Barbeau, H., and Rossignol, S. (1991). Initiation and modulation of the locomotor pattern in the adult chronic spinal cat by noradrenergic, serotonergic and dopaminergic drugs. Brain Res. *546*, 250–260.

41. Harris-Warrick, R.M., and Cohen, A.H. (1985). Serotonin modulates the central pattern generator for locomotion in the isolated lamprey spinal cord. J. Exp. Biol. *116*, 27–46.

42. Parker, D. (1995). Serotonergic modulation of locust motor neurons. J. Neurophysiol. *73*, 923–932.

43. Albin, S.D., Kaun, K.R., Knapp, J.-M., Chung, P., Heberlein, U., and Simpson, J.H. (2015). A Subset of Serotonergic Neurons Evokes Hunger in Adult Drosophila. Curr. Biol. *25*, 2435–2440.

44. Majeed, Z.R., Abdeljaber, E., Soveland, R., Cornwell, K., Bankemper, A., Koch, F., and Cooper, R.L. (2016). Modulatory Action by the Serotonergic System: Behavior and Neurophysiology in Drosophila melanogaster. Neural Plast. *2016*, 7291438.

45. Mohammad, F., Aryal, S., Ho, J., Stewart, J.C., Norman, N.A., Tan, T.L., Eisaka, A., and Claridge-Chang, A. (2016). Ancient Anxiety Pathways Influence Drosophila Defense Behaviors. Curr. Biol. *26*, 981–986.

46. Pooryasin, A., and Fiala, A. (2015). Identified Serotonin-Releasing Neurons Induce Behavioral Quiescence and Suppress Mating in Drosophila. J. Neurosci. *35*, 12792–12812.

47. Qian, Y., Cao, Y., Deng, B., Yang, G., Li, J., Xu, R., Zhang, D., Huang, J., and Rao, Y. (2017). Sleep homeostasis regulated by 5HT2b receptor in a small subset of neurons in the dorsal fan-shaped body of drosophila. eLife *6*. Published online October 6, 2017. https://doi.org/10.7554/eLife.26519.

48. Alekseyenko, O.V., Lee, C., and Kravitz, E.A. (2010). Targeted manipulation of serotonergic neurotransmission affects the escalation of aggression in adult male Drosophila melanogaster. PLoS ONE *5*, e10806.

49. Alekseyenko, O.V., Chan, Y.B., Fernandez, M.P., Bülow, T., Pankratz, M.J., and Kravitz, E.A. (2014). Single serotonergic neurons that modulate aggression in Drosophila. Curr. Biol. *24*, 2700–2707.

50. Riemensperger, T., Isabel, G., Coulom, H., Neuser, K., Seugnet, L., Kume, K., Iché-Torres, M., Cassar, M., Strauss, R., Preat, T., et al. (2011). Behavioral consequences of dopamine deficiency in the Drosophila central nervous system. Proc. Natl. Acad. Sci. USA *108*, 834–839.

51. Ueno, T., Masuda, N., Kume, S., and Kume, K. (2012). Dopamine modulates the rest period length without perturbation of its power law distribution in Drosophila melanogaster. PLoS ONE *7*, e32007.

52. Pendleton, R.G., Rasheed, A., Sardina, T., Tully, T., and Hillman, R. (2002). Effects of tyrosine hydroxylase mutants on locomotor activity in Drosophila: a study in functional genomics. Behav. Genet. *32*, 89–94.

53. Yang, Z., Yu, Y., Zhang, V., Tian, Y., Qi, W., and Wang, L. (2015). Octopamine mediates starvation-induced hyperactivity in adult Drosophila. Proc. Natl. Acad. Sci. USA *112*, 5219–5224.

54. Brembs, B., Christiansen, F., Pflüger, H.J., and Duch, C. (2007). Flight initiation and maintenance deficits in flies with genetically altered biogenic amine levels. J. Neurosci. *27*, 11122–11131.

55. Friggi-Grelin, F., Coulom, H., Meller, M., Gomez, D., Hirsh, J., and Birman, S. (2003). Targeted gene expression in Drosophila dopaminergic cells using regulatory sequences from tyrosine hydroxylase. J. Neurobiol. *54*, 618–627.

56. Cole, S.H., Carney, G.E., McClung, C.A., Willard, S.S., Taylor, B.J., and Hirsh, J. (2005). Two functional but noncomplementing Drosophila tyrosine decarboxylase genes: distinct roles for neural tyramine and octopamine in female fertility. J. Biol. Chem. *280*, 14948–14955.

57. Branson, K., Robie, A.A., Bender, J., Perona, P., and Dickinson, M.H. (2009). High-throughput ethomics in large groups of Drosophila. Nat. Methods *6*, 451–457.

58. Eyjolfsdottir, E., Branson, S., Burgos-Artizzu, X.P., Hoopfer, E.D., Schor, J., Anderson, D.J., and Perona, P. (2014). Detecting social actions of fruit flies. In from book Recognizing Complex Events in Videos by Learning Key Static-Dynamic Evidences, D. Fleet, T. Pajdla, B. Schiele, and T. Tuytelaars, eds. (Springer International Publishing), pp. 772–787.

59. Chen, C.-L., Hermans, L., Viswanathan, M.C., Fortun, D., Aymanns, F., Unser, M., Cammarato, A., Dickinson, M.H., and Ramdya, P. (2018). Imaging neural activity in the ventral nerve cord of behaving adult Drosophila. Nat. Commun. *9*, 4390.

60. Gibert, P., Huey, R.B., and Gilchrist, G.W. (2001). Locomotor performance of Drosophila melanogaster: interactions among developmental and adult temperatures, age, and geography. Evolution *55*, 205–209.

61. Cho, W., Heberlein, U., and Wolf, F.W. (2004). Habituation of an odorant-induced startle response in Drosophila. Genes Brain Behav. *3*, 127–137.

62. Lee, G., and Park, J.H. (2004). Hemolymph sugar homeostasis and starvation-induced hyperactivity affected by genetic manipulations of the adipokinetic hormone-encoding gene in Drosophila melanogaster. Genetics *167*, 311–323.

63. Yeomans, J.S., Li, L., Scott, B.W., and Frankland, P.W. (2002). Tactile, acoustic and vestibular systems sum to elicit the startle reflex. Neurosci. Biobehav. Rev. *26*, 1–11.

64. Yeomans, J.S., and Frankland, P.W. (1995). The acoustic startle reflex: neurons and connections. Brain Res. Brain Res. Rev. *21*, 301–314.

65. Card, G.M. (2012). Escape behaviors in insects. Curr. Opin. Neurobiol. *22*, 180–186.

66. Zacarias, R., Namiki, S., Card, G.M., Vasconcelos, M.L., and Moita, M.A. (2018). Speed dependent descending control of freezing behavior in Drosophila melanogaster. Nat. Commun. 9, 3697.

67. Card, G., and Dickinson, M.H. (2008). Visually mediated motor planning in the escape response of Drosophila. Curr. Biol. 18, 1300–1307.

68. Davis, M. (1984). The mammalian startle response. In Neural Mechanisms of Startle Behavior, R.C. Eaton, and M.A. Boston, eds., pp. 287–351, Springer.

69. Saudou, F., and Hen, R. (1994). 5-Hydroxytryptamine receptor subtypes in vertebrates and invertebrates. Neurochem. Int. 25, 503–532.

70. Tierney, A.J. (2018). Invertebrate serotonin receptors: a molecular perspective on classification and pharmacology. J. Exp. Biol. 221, jeb184838.

71. Saudou, F., Boschert, U., Amlaiky, N., Plassat, J.L., and Hen, R. (1992). A family of Drosophila serotonin receptors with distinct intracellular signalling properties and expression patterns. EMBO J. 11, 7–17.

72. Witz, P., Amlaiky, N., Plassat, J.L., Maroteaux, L., Borrelli, E., and Hen, R. (1990). Cloning and characterization of a Drosophila serotonin receptor that activates adenylate cyclase. Proc. Natl. Acad. Sci. USA 87, 8940–8944.

73. Blenau, W., Daniel, S., Balfanz, S., Thamm, M., and Baumann, A. (2017). Dm5-HT2B: Pharmacological Characterization of the Fifth Serotonin Receptor Subtype of *Drosophila melanogaster*. Front. Syst. Neurosci. 11, 28.

74. Colas, J.F., Launay, J.M., Kellermann, O., Rosay, P., and Maroteaux, L. (1995). Drosophila 5-HT2 serotonin receptor: coexpression with fushi-tarazu during segmentation. Proc. Natl. Acad. Sci. USA 92, 5441–5445.

75. Gnerer, J.P., Venken, K.J.T., and Dierick, H.A. (2015). Gene-specific cell labeling using MiMIC transposons. Nucleic Acids Res. 43, e56.

76. Veasey, S.C., Fornal, C.A., Metzler, C.W., and Jacobs, B.L. (1995). Response of serotonergic caudal raphe neurons in relation to specific motor activities in freely moving cats. J. Neurosci. 15, 5346–5359.

77. Veasey, S.C., Fornal, C.A., Metzler, C.W., and Jacobs, B.L. (1997). Single-unit responses of serotonergic dorsal raphe neurons to specific motor challenges in freely moving cats. Neuroscience 79, 161–169.

78. Correia, P.A., Lottem, E., Banerjee, D., Machado, A.S., Carey, M.R., and Mainen, Z.F. (2017). Transient inhibition and long-term facilitation of locomotion by phasic optogenetic activation of serotonin neurons. eLife 6. Published online February 14, 2017. https://doi.org/10.7554/eLife.20975.

79. Gibson, W.T., Gonzalez, C.R., Fernandez, C., Ramasamy, L., Tabachnik, T., Du, R.R., Felsen, P.D., Maire, M.R., Perona, P., and Anderson, D.J. (2015). Behavioral responses to a repetitive visual threat stimulus express a persistent state of defensive arousal in Drosophila. Curr. Biol. 25, 1401–1415.

80. Pearson, K.G., and O'Shea, M. (1984). Escape behavior of the locust. In Neural Mechanisms of Startle Behavior Neural Mechanisms of Startle Behavior., R.C. Eaton, and M.A. Boston, eds., pp. 163–178, Springer.

81. Ritzmann, R.E. (1984). The cockroach escape response. In Neural Mechanisms of Startle Behavior Neural Mechanisms of Startle Behavior., R.C. Eaton, and M.A. Boston, eds., pp. 93–131, Springer.

82. Davis, M., and Sheard, M.H. (1974). Habituation and sensitization of the rat startle response: effects of raphe lesions. Physiol. Behav. 12, 425–431.

83. Carlton, P.L., and Advokat, C. (1973). Attenuated habituation due to parachlorophenylalanine. Pharmacol. Biochem. Behav. 1, 657–663.

84. Davis, M., Strachan, D.I., and Kass, E. (1980). Excitatory and inhibitory effects of serotonin on sensorimotor reactivity measured with acoustic startle. Science 209, 521–523.

85. Astrachan, D.I., and Davis, M. (1981). Spinal modulation of the acoustic startle response: the role of norepinephrine, serotonin and dopamine. Brain Res. 206, 223–228.

86. Cande, J., Namiki, S., Qiu, J., Korff, W., Card, G.M., Shaevitz, J.W., Stern, D.L., and Berman, G.J. (2018). Optogenetic dissection of descending behavioral control in *Drosophila*. eLife 7. Published online June 26, 2018. https://doi.org/10.7554/eLife.34275.

87. Perrier, J.-F., and Cotel, F. (2015). Serotonergic modulation of spinal motor control. Curr. Opin. Neurobiol. 33, 1–7.

88. Johnson, M.D., and Heckman, C.J. (2014). Gain control mechanisms in spinal motoneurons. Front. Neural Circuits 8, 81.

89. Cappellini, G., Ivanenko, Y.P., Dominici, N., Poppele, R.E., and Lacquaniti, F. (2010). Motor patterns during walking on a slippery walkway. J. Neurophysiol. 103, 746–760.

90. Voloshina, A.S., and Ferris, D.P. (2015). Biomechanics and energetics of running on uneven terrain. J. Exp. Biol. 218, 711–719.

91. Nakazawa, K., Kawashima, N., Akai, M., and Yano, H. (2004). On the reflex coactivation of ankle flexor and extensor muscles induced by a sudden drop of support surface during walking in humans. J. Appl. Physiol. 96, 604–611.

92. Kavlie, R.G., and Albert, J.T. (2013). Chordotonal organs. Curr. Biol. 23, R334–R335.

93. Mamiya, A., Gurung, P., and Tuthill, J.C. (2018). Neural Coding of Leg Proprioception in Drosophila. Neuron 100, 636–650.

94. Daniels, R.W., Gelfand, M.V., Collins, C.A., and DiAntonio, A. (2008). Visualizing glutamatergic cell bodies and synapses in Drosophila larval and adult CNS. J. Comp. Neurol. 508, 131–152.

95. Ryder, E., Blows, F., Ashburner, M., Bautista-Llacer, R., Coulson, D., Drummond, J., Webster, J., Gubb, D., Gunton, N., Johnson, G., et al. (2004). The DrosDel collection: a set of P-element insertions for generating custom chromosomal aberrations in Drosophila melanogaster. Genetics 167, 797–813.

96. Enriquez, J., Venkatasubramanian, L., Baek, M., Peterson, M., Aghayeva, U., and Mann, R.S. (2015). Specification of individual adult motor neuron morphologies by combinatorial transcription factor codes. Neuron 86, 955–970.

97. Burgos, A., Honjo, K., Ohyama, T., Qian, C.S., Shin, G.J.-E., Gohl, D.M., Silies, M., Tracey, W.D., Zlatic, M., Cardona, A., and Grueber, W.B. (2018). Nociceptive interneurons control modular motor pathways to promote escape behavior in *Drosophila*. eLife 7. Published online March 12, 2018. https://doi.org/10.7554/eLife.26016.

98. Klapoetke, N.C., Murata, Y., Kim, S.S., Pulver, S.R., Birdsey-Benson, A., Cho, Y.K., Morimoto, T.K., Chuong, A.S., Carpenter, E.J., Tian, Z., et al. (2014). Independent optical excitation of distinct neural populations. Nat. Methods 11, 338–346.

99. Hardie, R.C., Raghu, P., Moore, S., Juusola, M., Baines, R.A., and Sweeney, S.T. (2001). Calcium influx via TRP channels is required to maintain PIP2 levels in Drosophila photoreceptors. Neuron 30, 149–159.

100. Shearin, H.K., Macdonald, I.S., Spector, L.P., and Stowers, R.S. (2014). Hexameric GFP and mCherry reporters for the Drosophila GAL4, Q, and LexA transcription systems. Genetics 196, 951–960.

101. Schindelin, J., Arganda-Carreras, I., Frise, E., Kaynig, V., Longair, M., Pietzsch, T., Preibisch, S., Rueden, C., Saalfeld, S., Schmid, B., et al. (2012). Fiji: an open-source platform for biological-image analysis. Nat. Methods 9, 676–682.

102. Straw, A.D., and Dickinson, M.H. (2009). Motmot, an open-source toolkit for realtime video acquisition and analysis. Source Code Biol. Med. 4, 5.

103. Simon, J.C., and Dickinson, M.H. (2010). A new chamber for studying the behavior of Drosophila. PLoS ONE 5, e8793.

STAR★METHODS

KEY RESOURCES TABLE

REAGENT or RESOURCE	SOURCE	IDENTIFIER
Antibodies		
Rabbit anti Vglut; 1:10,000	Aaron DiAntonio [94]	N/A
Rabbit anti 5-HT; 1:1000	Millipore Sigma	RRID:AB_477522
Mouse anti TH; 1:1000	Immunostar	RRID:AB_572268
Mouse anti ChAT4B1; 1:500	Developmental Studies Hybridoma Bank (DSHB)	RRID:AB_528122
Mouse anti nc82 c; 1:20 – 1:100	DSHB	RRID:AB_2314866
Rabbit anti GABA; 1:1000	Millipore Sigma	RRID:AB_477652
Rabbit anti Tdc2; 1:200	Cova Labs	pab0822-P
Rabbit anti dsRed; 1:1000	Takara Bio	RRID:AB_10013483
Experimental Models: Strains of *D. melanogaster*		
; ; Trh Gal4	Bloomington Drosophila Stock Center (BDSC) [48]	RRID:BDSC_38389
; ; TH Gal4	BDSC [55]	RRID:BDSC_8848
; Tdc2 Gal4 ;	BDSC [56]	RRID:BDSC_9313
w^{1118} ; IIiso ; IIIiso	BDSC [95]	RRID:BDSC_5905
w^{1118} ; IIiso ; Trh-Gal4	This study	N/A
w^{1118} ; IIiso ; TH-Gal4	This study	N/A
w^{1118} ; Tdc2 Gal4 ; IIIiso	This study	N/A
w^{1118} ; IIiso ; Trh iso Gal4; outcrossed 10 x to w^{1118} ; IIiso ; IIIiso	This study	N/A
; UAS-mCD8::GFP;	[96]	N/A
tub > gal80 > ; tsh-LexA, LexAop-Flp ;; Tsh LexA made by Julie Simpson. Combined tool provided by Wes Grueber	[97]	N/A
; tsh-Gal80 ;	Julie Simpson	N/A
; ; UAS-csChrimson::mVenus	BDSC [98]	RRID:BDSC_55136
; ; UAS-Kir2.1	BDSC [99]	RRID:BDSC_6595
; ; 20XUAS-hexameric-GFP	BDSC / Steve Stowers [100]	RRID:BDSC_52262
; UAS-OpGCamp6f ; UAS-tdTomato	Pavan Ramdya [59]	N/A
IsoCS	Yi Rao [47]	N/A
w+ 5-HT1A^{Gal4} ;	Yi Rao [47]	N/A
w+ 5-HT1B^{Gal4} ;	Yi Rao [47]	N/A
w+; ; 5-HT2A^{Gal4}	Yi Rao [47]	N/A
w+; ; 5-HT7^{Gal4}	Yi Rao [47]	N/A
w+; ; Trh^{01}	Yi Rao [47]	N/A
; 5-HT1A-Gal4 (MI04464);	Herman A. Dierick [75]	N/A
; 5-HT1B-Gal4 (MI05213);	Herman A. Dierick [75]	N/A
; ; 5-HT2A-Gal4 (MI00459)	Herman A. Dierick [75]	N/A
; ; 5-HT2A-Gal4 (MI03299)	Herman A. Dierick [75]	N/A
; ; 5-HT2B-Gal4 (MI05208)	Herman A. Dierick [75]	N/A
; ; 5-HT2B-Gal4 (MI06500)	Herman A. Dierick [75]	N/A
; ; 5-HT2B-Gal4 (MI07403)	Herman A. Dierick [75]	N/A
; ; 5-HT7-Gal4 (MI00215)	Herman A. Dierick [75]	N/A
Vglut>>LexAVP16, LexO-CD8GFP /FM7; Vglut>>LexAVP16, UASFlp, LexO-CD8GFP /CyO; LexO-CD8GFP, LexO-CD8GFP, Vglut>>LexAVP16 /TM2	Myungin Baek	N/A
; Mhc-RFP ;	BDSC	RRID:BDSC_38464

(Continued on next page)

Continued

REAGENT or RESOURCE	SOURCE	IDENTIFIER
Software and Algorithms		
Fiji	[101]	https://fiji.sc
Caltech FlyTracker	[58]	http://www.vision.caltech.edu/Tools/FlyTracker/index.html
Flywalker	[25]	N/A
Flycapture		https://www.flir.com/products/flycapture-sdk
Fview2	Andrew Straw, modified from [102]	N/A
MATLAB 2018a	Mathworks	https://www.mathworks.com/products/matlab.html
R Studio 3.3.2		https://www.rstudio.com
Python 2.7 Anaconda		https://www.anaconda.com/distribution/
NIS Elements AR	Nikon	https://www.microscope.healthcare.nikon.com/products/software/nis-elements
PuTTY		https://www.chiark.greenend.org.uk/~sgtatham/putty/
Arduino IDE 1.8.5	Arduino	https://www.arduino.cc/en/Main/Software
Deposited Data and Code		
Code_data.zip	Zenodo.org	https://doi.org/10.5281/zenodo.3497587

LEAD CONTACT AND MATERIAL AVAILABILITY

Further information and requests for resources and reagents should be directed to and will be fulfilled by the Lead Contact, Richard Mann (rsm10@columbia.edu).

Fly lines generated by this study are available upon request.

EXPERIMENTAL MODEL AND SUBJECT DETAILS

Fly Husbandry
Experimental model for this study was the vinegar fly *Drosophila melanogaster.* A full list of strains used in the paper is included in the Key Resource Table. Unless otherwise described, flies were maintained at 25°C on dextrose cornmeal food using standard laboratory techniques.

Animal Rearing for Behavioral Experiments
For Flywalker experiments, flies were maintained on dextrose cornmeal food at 25°C. For arena experiments, flies were maintained on Nutrifly German Sick food (Genessee Scientific 66-115) in an incubator humidified at 60% with a 12h:12h light:dark cycle. Crosses used for behavioral experiments were flipped every 2-3 days to prevent overcrowding. As animals eclosed, females of the appropriate genotype were collected under CO_2 anesthesia every 2-3 days. Females were used for all experiments due to their larger size which facilitated accurate tracking. For non-optogenetic experiments, flies were collected onto Nutrifly Food without any additive. For optogenetic experiments, flies were collected onto Nutrifly food supplemented with 0.4 mM ATR dissolved in EtOH or an equal concentration of solvent alone (for arena experiments), or corn food supplemented with 0.4mM ATR dissolved in DMSO or an equal concentration of solvent alone for Flywalker experiments. Animals were aged in the dark (for optogenetic experiments) or on the same light:dark cycle for 2-3 more days at 25°C before being assayed. Gal4 driver lines used for arena experiments had been outcrossed ten times to an isogenized *w1118* control population. Gal4 driver lines used for Flywalker experiments had been isogenized on two chromosomes, but not on the chromosome containing the Gal4 transgene. For a complete list of lines used in this paper please refer to the Key Resources Table.

Fly Genotypes with Associated Figures

Experimental Line	Main Figure	Supplementary
+ /+ tsh Gal80 / UAS mCD8 GFP ; Trh Gal4 / +	Figures 1B, 1B′, 1B″	
tub > gal80 > / + tsh LexA, lexAop Flp / + Trh Gal4 / UAS mCD8 GFP	Figures 1C, C′, C″	
+ /+ tsh Gal80 / +; UAS mCD8 GFP, TH Gal4 / +	Figures 1D, D′, D″	

(Continued on next page)

Continued

Experimental Line	Main Figure	Supplementary
tub > gal80 > / + tsh LexA, lexAop Flp / + TH Gal4, UAS mCD8 GFP / +	Figures 1E, E′, E″	
+ /+ tsh Gal80 / Tdc2 Gal4 ; UAS mCD8 GFP / +	Figures 1F, F′ F″	
tub > gal80 > / + tsh LexA, lexAop Flp / Tdc2 Gal4 ; UAS mCD8 GFP / +	Figures 1G, G′, G″	
tub > gal80 > / w^{1118} ; tsh LexA, lexAop Flp / isoII ; UAS csChrimson::mVenus / isoIII	Figures 1H, 2A, and 2C	Figures S2D and S2F
tub > gal80 > / w^{1118} ; tsh LexA, lexAop Flp / isoII ; UAS csChrimson::mVenus / Trh Gal4	Figures 1H and 3A–3M	Figure S3D
		Figure S4B
tub > gal80 > / w^{1118} ; tsh LexA, lexAop Flp / isoII ; UAS csChrimson::mVenus / TH Gal4	Figure 1H	
tub > gal80 > / w^{1118} ; tsh LexA, lexAop Flp / Tdc2 Gal4 ; UAS csChrimson::mVenus / isoIII	Figure 1H	
tub > gal80 > / w^{1118} ; tsh LexA, lexAop Flp / isoII ; UAS csChrimson::mVenus / Trh iso Gal4	Figures 2A and 2C	Figure S1
		Figures S2D, S2F, S2H, and S2I
tub > gal80 > / w^{1118} ; tsh LexA, lexAop Flp / isoII ; UAS Kir2.1::GFP / isoIII	Figures 2B, 2C, and 4	Figures S2E and S2G
tub > gal80 > / w^{1118} ; tsh LexA, lexAop Flp / isoII ; UAS Kir2.1::GFP / Trh iso Gal4	Figures 2B, 2C, and 4	Figures S2E and S2G–S2I
		Figure S5C
tub > gal80 > /+ tsh-LexA, lexAop-FLP/UAS-opGCaMP6f; Trh-Gal4/UAS-tdTomato	Figures 2D–2F	Figures S4B, S4C, S4E, and S4F
isoCS	Figures 5A–5G	Figures S5A and S5B
W+ ; 5-HT1A^{Gal4} ; +	Figures 5A, 5F, and 5G	Figures S5A and S5G
W+ ; 5-HT1B^{Gal4} ; +	Figures 5A, 5D, and 5G	Figures S5A and S5E
W+ ; + ; 5-HT2A^{Gal4}	Figures 5A, 5E, and 5G	Figures S5A and S5F
W+ ; + ; 5-HT7^{Gal4}	Figures 5A, 5C, and 5G	Figures S5A and S5D
W+ ; + ; Trh^{01}	Figures 5A–5F and 5G	Figures S5A–S5G
5-HT1A-Gal4 (MI04464) / + ; 20X-UAS hexameric GFP / +	Figures 6A and 6G	Figure S6G
5-HT1B-Gal4 (MI05213) / + ; 20X-UAS hexameric GFP / +	Figures 6B and 6H	Figure S6G
+/+ ; 5-HT2A-Gal4 (MI00459) / 20X-UAS hexameric GFP	Figures 6C and 6I	Figure S6G
+/+ ; 5-HT2B-Gal4 (MI05208) / 20X-UAS hexameric GFP	Figures 6D and 6J	Figure S6G
+/+ ; 5-HT7-Gal4 (MI0215) / 20X-UAS hexameric GFP	Figures 6E and 6K	Figure S6G
+/+ ; 5-HT2A-Gal4 (MI03299) / 20X-UAS hexameric GFP		Figure S6G
+/+ ; 5-HT2B-Gal4 (MI06500) / 20X-UAS hexameric GFP		Figure S6G
+/+ ; 5-HT2B-Gal4 (MI07403) / 20X-UAS hexameric GFP		Figure S6G
Vglut>>LexA, LexO-CD8GFP / +; Vglut>>LexA, UASFlp, LexO-CD8GFP / +; LexO-CD8GFP, LexO-CD8GFP, Vglut>>LexAVP16 / 5-HT2B-Gal4 (MI05208)		Figure S6A
Vglut>>LexA, LexO-CD8GFP / +; Vglut>>LexA, UASFlp, LexO-CD8GFP / +; LexO-CD8GFP, LexO-CD8GFP, Vglut>>LexAVP16 / 5-HT7-Gal4 (MI0215)		Figure S6B
Vglut>>LexA, LexO-CD8GFP / +; Vglut>>LexA, UASFlp, LexO-CD8GFP / MHC-RFP; LexO-CD8GFP, LexO-CD8GFP, Vglut>>LexAVP16 / 5-HT2B-Gal4 (MI05208)		Figure S6C
Vglut>>LexA, LexO-CD8GFP / +; Vglut>>LexA, UASFlp, LexO-CD8GFP / MHC-RFP; LexO-CD8GFP, LexO-CD8GFP, Vglut>>LexAVP16 / 5-HT7-Gal4 (MI0215)		Figure S6D

METHOD DETAILS

Immunostaining Brain and VNC

Brains and VNCs were dissected in phosphate buffered saline with 0.3% Triton (PBST) and fixed in 4% Paraformaldehyde (PFA) for 20 minutes. Samples were washed five times for 20 minutes in PBST with 0.1% Bovine serum albumin (BSA), and then blocked in PBST-BSA for one hour at room temperature, or overnight at 4°C. Samples were incubated with primary antibody diluted in PBST-BSA overnight at 4°C, and washed five times 20 minutes with PBST-BSA the next day. Primary antibodies used were: anti-VGlut (gift from Aaron DiAntonio, described in [94]); anti-5HT (1:1000 Sigma); anti-TH (1:1000 Immunostar); anti-ChAT (1:500 DSHB); anti-Brp (1:50-1:100 DSHB); anti-GABA (1:1000 Sigma); anti-Tdc2 (1:200 Cova Labs). Samples were then incubated in secondary antibody diluted in PBST-BSA overnight at 4°C. Secondary antibodies used Goat Anti-Rabbit Alexa 555 (1:500 Invitrogen); Donkey Anti-Mouse 647 (1:500 Jackson Immunolabs);

Goat Anti-Mouse 555 (1:500 Life Technologies). The next day, samples were washed five times for 20 minutes in PBST, and then the liquid was replaced with Vectashield and samples were incubated overnight prior to mounting. Brains and VNCs from the same animals were mounted together, with the ventral surface of the VNC and the anterior surface of the brain facing up.

Validation of expression patterns during two photon experiments were performed as described in [59]. Briefly, brains and VNCs were dissected out of the animal, and fixed in 4% PFA for 20 min at room temperature. Samples were washed 2-3 × 10-15 min in 1% PBST and blocked for one hour at room temperature in 1% PBST with 5% NGS. Samples were stained overnight at room temperature with primary antibody diluted in blocking solution. Primary antibodies used included anti-Brp (1:20 DSHB anti-dsRed (1:1000 Takara Bio). The next day, samples were washed 2-3 × 10-15 min in 1% PBST. Samples were incubated with secondary antibody overnight at room temperature in the dark. Secondaries included Goat Anti-Rabbit Cy3 (1:400 Jackson); Goat Anti-Mouse 633 (Thermofisher). The next day, samples were washed 2-3 × 10-15 min 1% PBST and mounted dorsal side up in Slow Fade Gold mounting medium (ThermoFisher).

Confocal Imaging of Brains and VNCs

Mounted brains and VNCs were imaged on a Leica TCS SP5 confocal at 20X magnification with a resolution of 1024 × 512 pixels, and at a scanning rate of 200 Hz and 3x averaging. Sections were taken at 1 μm increments. Laser power and detector gain were maintained constant for the brain and VNC of the same animals, but were adjusted for optimal signal between animals.

Imaging of fixed samples following two photon live imaging experiments was performed as described in [59] on a Zeiss LSM 700 Laser Scanning Confocal Microscope at 20X magnification and 2X averaging, with a 0.52 X 0.52 μm pixel size. Z sections were taken at 1 μm intervals.

Cell Counting and Quantification

Images were analyzed in Fiji [101]. For quantification of the number of cells driven by *Trh-Gal4* in the brain and VNC, mVenus or GFP positive and 5-HT positive cell bodies were counted from five or more individual animals.

Leg Dissection, Imaging, and Image Processing

To prepare legs for imaging, fly heads and abdomens were removed, and thoraces with legs attached were fixed overnight in 4% PFA at 4°C. Carcasses were washed 5x with 0.03% PBST, and then placed in Vectashield overnight before legs were mounted. Imaging was performed on a Leica SP5 confocal at 20X magnification and 1024 × 1024 pixel resolution with 3x averaging, and Z sections were taken at 1 μm. Two PMT detectors were set to capture green fluorescent signal and the green autofluorescence of the cuticle. Laser power was adjusted independently for each line to achieve optimal visualization of structures. Images were processed in Fiji [101]. Autofluorescence was subtracted from the green channel to allow for clearer visualization of leg structures.

Arena Experiments
Hardware

The skeleton of the system was built of 80-20 bars and acrylic plates and the arena itself was machined out of polycarbonate to the specifications published in [103]. The polycarbonate plastic arena was embedded in an aluminum plate to maintain a level surface. During experiments, the arena was covered with an acrylic disc with a small hole for mouth pipetting in flies. The inside of the lid was coated in a thin layer of Fluon (Amazon, B00UJLH12A) to prevent flies from walking on the ceiling.

A Point Grey Blackfly Mono USB3 camera fitted with a Tamron 1/2" F/1.2 IR C-mount lens (B&H photo) was mounted above the arena and connected by USB 3 cable to a System 76 Leopard WS computer running Ubuntu 14.04 LTS. A Kodax 3x3" 89B Opaque IR filter (B&H photo) was placed in front of the camera detector to allow for detection of IR but not visible light.

Backlighting and optogenetic stimulation was provided by a plate of LEDs sitting under the arena. An acrylic diffuser was placed between the lighting plate and the arena. Each plate was designed with two sets of LEDs – one for IR backlighting (ledlightsworld.com SMD3528-300) and one for optogenetic or white light stimulation (superbrightLEDS.com NFLS-x-LC2 in Red or Natural White). These plates were swapped out when experiments required different color LEDs. To allow for detection of the on state of non-IR lights, an additional IR light was wired in series with each visible light array, and placed within the field of view of the camera.

Each set of lights was powered separately by an Arduino Uno driver, allowing for modulation of light intensity via Pulse Width Modulation (PWM). Commands to set LED brightness and start and end experiments were sent to this driver using a PuTTY terminal and USB serial interface. For all the experiments described here, both IR and visible spectrum LEDs were set at 100% brightness. At the center of the arena this corresponded roughly to intensities of:

Light On	Percent	Intensity	Wavelength Measured
Infrared	100	.13 mW	1050 nm
		.08 mW	635 nm
		.08 mW	535 nm
Infrared + Red	100	.6 mW	635 nm
Infrared + White	100	.62 mW	635 nm
		.68 mW	535 nm

Data Acquisition

All behavioral recordings were done during the three-hour morning activity peak. Prior to the experiment, the arena was leveled, the lid cleaned, and a new layer of Fluon applied. For each experiment, videos were recorded of cohorts of 10 flies. For each recording session, flies were mouthpipetted into the arena through a small hole and then the arena lid was slid to move the hole out of the field of view. A blackout curtain cover (Thor Labs, BK5) was used to surround the arena, protecting it from any contaminating light.

Experimental protocols were programmed into the Arduino through serial communication via a PuTTY terminal. Videos were recorded at a rate of 30 frames per second and stored in a compressed "fly movie format" using custom software written by Andrew Straw at the University of Freiberg based on work previously described [102].

Orientation

For inverted experiments, animals were introduced into the arena set-up when it was upright, and the lid of the arena was taped in place. The entire arena was manually inverted and propped up on two overturned ice buckets. Flies were either recorded upright and then inverted, for five minutes each, or in the opposite order.

Starvation

24 hours prior to behavioral assay, half of the flies were transferred to an empty tube with a wet Kim Wipe. Behavioral recordings were collected as described above and lasted for five minutes.

Heat

Heated experiments were carried out inside a walk-in temperature-controlled incubator, which was set at either 18, 25, 30, or 37°C and 40% humidity. Flies were introduced to the arena immediately after entering the temperature-controlled room, recording began immediately thereafter and lasted for five minutes.

Light

For experiments examining responses to light stimuli, flies were first exposed to five minutes of white light, and then a one minute period of darkness.

Vibration

To provide a vibration stimulus, four 3V haptic motors (1670-1023-ND, Digikey) were attached to the aluminum plate in which the arena sat using 3D printed holders. The motors were wired in series and driven by the same Arduino system driving the arena's LED lighting array. For all experiments described, vibration was set at 10% power. The protocol for vibration experiments consisted of a brief habituation period (five minutes for inactivation experiments, 30 s for mutant experiments) followed by a 10 s vibration pulse and a 110 s recovery period.

Flywalker Experiments

Hardware

The Flywalker was constructed as described in [25] with modifications. The rig consisted of a frame of 80/20 supporting a sheet of 6 mm Borofloat optical glass with polished edges placed over an Andor Zyla 4.2 Magapixel sCMOS camera with an AF Nikkor 24-85mm 1:2.8-4 D lens (Nikon). On each edge of the glass were placed four Luxeon Neutral White (4100K) Rebel LED on a SinkPAD-II 10mm Square Base (230 lm @ 700mA) wired in series. Each set of lights was driven by a dedicated 700mA, Externally Dimmable, BuckPuck DC Driver (Luxeon), and all four of these drivers were connected to a single power supply. Each driver was independently adjustable.

Chambers were 3D printed by Protolabs (schematics available upon request). The ceiling and walls of the chamber were painted with Fluon mixed with india ink, to prevent flies from walking on the ceiling while maintaining an effective dark background. Small far-red LEDS were embedded in the walls of the chamber for Chrimson optogenetic experiments (LXM3-PD01 LUXEON). These lights were controlled by an Arduino driver that used pulsewitdth modulation to adjust light brightness. Commands were sent to this driver using a PuTTY terminal and USB serial interface. For all the experiments described here, LEDs were set at 20% brightness.

Data Acquisition

The Flywalker was calibrated using a calibration reticle prior to use on each day. On the day of the experiment, animals were mouthpipetted into a clean glass tube and allowed to equilibrate for five minutes to get rid of as much dirt and food as possible, to prevent contamination of the glass surface. 2-3 flies were added to the chamber by mouth pipette.

Videos were recorded using the NIS Elements AR software. A constant region of interest was defined such that the rate of recording was 226 fps. Each group of animals was recorded for one minute. Videos were cut to select traces where flies walked straight without touching the wall for > 6 steps without other flies in the frame.

Functional Imaging Experiments

Functional imaging experiments on *Trh ∩ tsh > opGCaMP6f, tdTomato* animals were performed as described in [59].

QUANTIFICATION AND STATISTICAL ANALYSIS

Arena Experiments

Tracking

Videos were tracked using the FlyTracker software from the Caltech vision lab [58]. Prior to tracking, pixel to mm conversion was calibrated using an inbuilt GUI. One calibration file was generated for all videos taken on the same day. Background model and

thresholds were adjusted to provide optimal recognition of animals and were not standardized between recording sessions. If present, the state of an indicator light was annotated by custom-written MATLAB software.

Behavioral classifiers

Each frame of an individual's walking bout was assigned a behavioral classifier based on the definitions below:

Jump: Jumps were classified as frames where the velocity of the animal exceeded 50 mm/s.
Walk: Walking frames were defined using a dual threshold Schmitt trigger filter. Speed thresholds were set at 1 and 2.5 mm/s, and time thresholds were 0.1 s. Walking frames were also specified to be those in which the fly was not already engaged in a jump.
Stop: Stop frames were classified as any frames where animals were not performing walking or jumping behaviors.

Parameters

Baseline walking parameters:

Walk Frequency: the percent of frames classified as walking during the recording period.
Overall Velocity: the median of all velocities over the recording period.
Walking Velocity: the median of velocities during all frames when the animal is classified as walking.
Maximum Walking Velocity: the maximum velocity an animal reaches during walking.
Angular velocity: the median value of angular velocity. This parameter takes into account directionality of turning.
Absolute Angular Velocity: the median of the absolute value of angular velocities. This parameter does not take into account directionality of turning.
Distance from Wall: the median distance from the closest point on the arena wall during the recording period.
Walking bout number: bouts were defined as contiguous frames of walking (longer than 0.1 s as specified in the walking classifier). The number of bouts was calculated for the entire recording period.
Walking bout duration: the length of each bout was calculated, and the median of all bout lengths was taken for each animal.
Stop bout number and duration: calculated as for walking bouts.
Jump Frequency: the percent of time that an animal spends in the jump state as defined above.

Startle parameters:

Startle responses were highly variable between individuals. To generate smoother average traces and model fitting, the data was serially resampled, with the median velocity of 20 animals selected for each frame, generating an average trace of random animals each run. The number of resampling runs for each genotype matched the actual number of animals studied.

Parameters calculated for each averaged trace included:

Minimum Velocity: defined as the minimum velocity reached within the first three seconds of the walking bout. This time threshold was selected based on aggregate traces that show the initial pause phase is well below this threshold.
Maximum Velocity: defined as the maximum velocity reached during the vibration stimulus period.
Pause Length: a Schmitt trigger classifier was used to define pause bouts. For inactivation light data and mutant vibration data, speed thresholds were defined as 2 mm/s faster than the minimum speed, and 5 mm/s faster than the minimum speed. For inactivation vibration data thresholds were 2 mm/s faster than the minimum speed and 3 mm/s faster than the minimum speed. Time thresholds were defined as 0.17 s for the "not paused" classification. No constraints were set on the length of the pause phase. The length of the first pause bout after the onset of the stimulus was recorded as "pause length." The thresholds of the classifier were tested with ten average traces per genotype and classifier fit was validated by eye.
Rise Time: defined as the time from the end of the pause phase to the maximum speed during the vibration pulse.

Statistics

For optogenetic arena experiments, behavior parameters described above were calculated for the five-minute light on period and compared to the same metric calculated during the light off period for each individual. For each activation experiment, we recorded behavior from both experimental (*Trh* ∩ *tsh* > *csChrimson*) and control (w^{1118} ∩ *tsh* > *csChrimson*) flies. For each genotype, we analyzed data from flies that had been fed with ATR, the required co-factor for optogenetic activation, and flies from the same cross that had been fed on food depleted of ATR. Figures show comparisons between ATR+ control and experimental animal behavior, as we found these populations had the most similar light off behavior pattern. However, significant differences in parameters are consistent even when all controls are included in the analysis.

For constitutive inhibition arena experiments, behavior during the five-minute light off period was analyzed for experimental (*Trh* ∩ *tsh* > *Kir2.1*) and control (w^{1118} ∩ *tsh* > *Kir2.1*) flies fed on the same ATR negative food we used for optogenetic experiments.

All analysis on data from arena experiments was performed in MATLAB using custom-written scripts. For each individual and parameter, a Z score was calculated comparing that individual's behavior to the mean and standard deviation of the control group. Z scores of different genotypes were compared using Kruskal-wallis analysis with Dunn-sidak multiple correction testing when multiple groups were being compared. To compare changes in velocity distribution, bootstrapping (1000 replicates) was used to estimate the median difference between two genotypes and fit a 95% confidence interval around this difference.

For experiments under different conditions (heat, orientation, starvation, vibration), median walking speed was compared between control and experimental animals under each condition using Kruskal-wallis analysis. For all conditions except vibration, animals who spent less than 30 s of the five minute recording period walking were excluded from the analysis. The response of each genotype to contextual shifts was independently assessed by Kruskal-wallis analysis with Dunn-sidak correction for multiple comparions.

As described above, for vibration and light experiments, parameters were defined for each average trace, with the number of traces per genotype corresponding to the actual number of animals in the experimental group. For a particular parameter, genotypes were compared using Kruskal Wallis test with subsequent Dunn-sidak correction for multiple comparisons. The model and statistical analysis was run ten times for each dataset to identify parameters that consistently were found to be significant.

The statistical tests performed for specific experiments are described in the figure legend for each experiment.

Flywalker Experiments
Tracking
Flywalker videos were automatically tracked using custom software written by Imre Bartos as described in [25]. Tracking was then validated by eye and incorrect footprint calls were corrected. Summary plots were then screened by eye for gross errors and for linear traces. If traces were short (< 3 traces per foot) or excessively turning, they were excluded.
Parameters
Behavioral parameters were calculated as described in [25]. Gait parameters were defined as follows. Leg order in combination: LF RF LM RM LH RH. 1 indicates the leg is in stance phase, 0 indicates the leg is in swing phase.

Tripod	Tetrapod	Wave	Non-Canonical
100110	011011	011111	All Other
011001	011110	101111	
	100111	110111	
	110110	111011	
	101101	111101	
	111001	111110	

Statistics
For Flywalker experiments, behavior was recorded for a one minute walking bout with red light illumination. Light off conditions were not possible as the white light LEDs required to generate fTIR signal contained the red wavelength used to activate our optogenetic tool. For each activation experiment, we recorded behavior from both experimental (*Trh – or other neuromodulatory Gal4 driver –* ∩ *tsh > csChrimson*) and control (*w^{1118}* ∩ *tsh > csChrimson*) flies. For each genotype, we analyzed data from flies that had been fed with ATR, the required co-factor for optogenetic activation, and flies from the same cross that had been fed on food depleted of ATR. Figures show comparisons between ATR+ and ATR- controls, as these populations provide the best genetic control and had the most similar behavioral pattern. However, significant differences in parameters are consistent even when all controls are included in our multivariate model (described below).

Statistical analysis of Flywalker data was performed using custom scripts written in MATLAB and R. For each walking bout, an average was calculated for every parameter across three to five footprints per leg. For parameters that exponentially related to speed, the natural logarithm was taken of both the bout speed and parameter values. A multivariable regression model was then run on the data for every kinematic parameter. The formula for this model was as follows:

$$y \sim \text{speed} * \text{ATR}$$

This model was designed to analyze the effects of activation while controlling for speed, which is the largest contributor to behavioral shifts.

We also ran a version of this model that contained all control data, to validate our results:

$$y \sim \text{speed} * \text{Genotype} * \text{ATR}$$

To prevent model overfitting, we selected our model based on Akaike information criterion using the R step() package.

Functional Imaging Experiments
Analysis

Initial image Processing: TIFF videos from two-photon microscopy were processed in Fiji to merge green (opGCaMP6f) and red (tdTomato) channels [101]. No brightness or contrast adjustments were performed, in order to standardize region-of-interest (ROI) selection.

ROI Selection: The tdTomato channel was used to select ROIs containing neuronal processes, using custom Python software relying on OpenCV and Numpy libraries. Images were converted into 8-bits, color ranges were extended, and contrast was augmented to better detect ROIs. Baseline signals were subtracted and then brightness was scaled to a maximum value of 255. A blur filter was applied to the image (blur value = 10), and then an Otsu Threshold was applied to binarize the grayscale image. After the image was thus thresholded, an erosion function (kernel size 5) was used to avoid the detection of overly large or small ROIs. The contours of all ROIs were detected on the eroded image and a copy of the contrast-augmented image was returned with ROI contours drawn super-imposed. A minimum threshold of 150 pixels was set on the ROI size to avoid overly small detections.

Fluorescence extraction: Mean fluorescence values for the tdTomato, or opGCaMP6f channels were calculated over all ROIs combined. Baseline signals for dF/F calculations were defined as mean raw fluorescence binned over 2.5 s.

Synchronization: Fluorescence measurements, behavior videography, and optic flow of spherical treadmill rotations were all recorded at different frame rates. Thus, we used interpolation to upsample fluorescence signals and behavioral videography acquisition rates to that of optic flow. Optic flow and fluorescence data were then smoothed (window size 200 ms). Optic flow data was then translated into mm/s in the anterior-posterior and medial-lateral directions and into degrees/s for yaw.

Automatic Walking Classifier: An automatic walking classifier was used to define walking bouts. A velocity of 0.31 mm/s was empirically determined as a threshold for distinguishing between walking and standing. The minimum threshold for bout length was empirically set to 2 s.

Manual behavioral annotation: Videos showing a side view of the fly on the spherical treadmill were manually annotated to capture four behaviors: (1) walk, (2) stop, (3) proboscis extension reflex, and (4) groom. All frames that could not neatly be classified as one of these four behaviors were defined as (5) other.

Statistics

Manually Annotated Behaviors: For each animal, the average dF/F for frames labeled a particular behavior classification was calculated. Comparisons between behaviors were made using Kruskal-Wallis testing with Dunn's correction for multiple comparisons.

Time courses: For each behavioral classification, an average time course was determined for each animal by averaging dF/F for all behavioral bouts (between 80 and 130 bouts per animal), centering them on bout onset. Averages across all animals were then calculated, and 95% confidence intervals fit by bootstrapping.

Correlation Analysis: A Pearson R correlation coefficient was calculated between walking velocity and dF/F.

DATA AND CODE AVAILABILITY

Tracking of flies in Flywalker and arena experiments was done using published tracking code [25, 58]. Analysis performed on Flywalker data was completed in R. Analysis performed on arena datasets was completed in MATLAB. Analysis of functional imaging data was completed in Python. Custom scripts written for these analyses and associated data are available for download at Zenodo. org: https://doi.org/10.5281/zenodo.3497586.